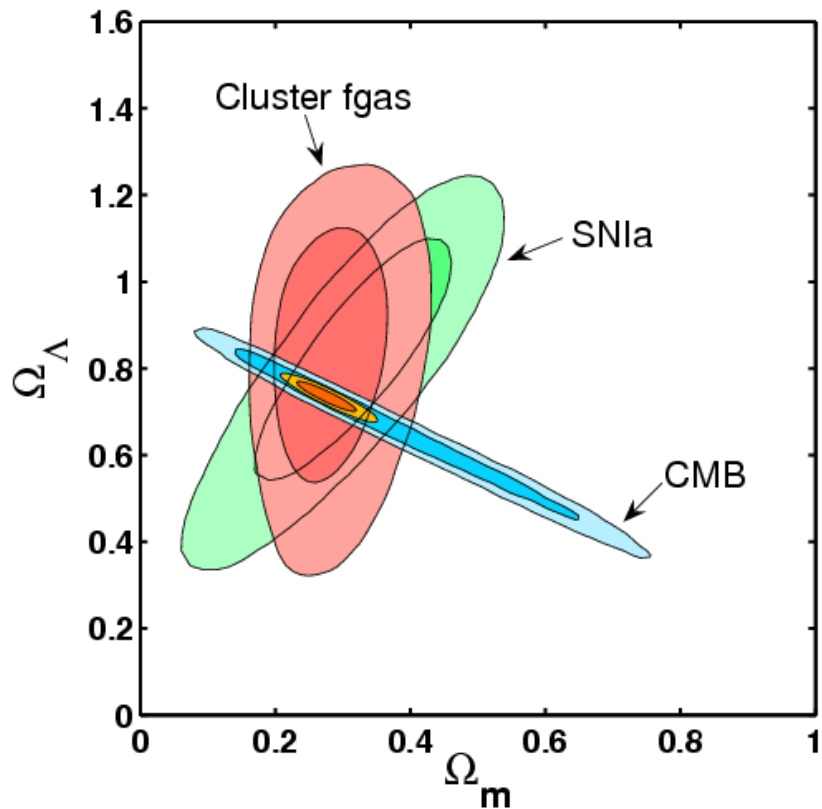


Dark matter in galaxy clusters

Steve Allen, KIPAC



In collaboration with:

David Rapetti (KIPAC)
Adam Mantz (KIPAC)
Robert Schmidt (Heidelberg)
Harald Ebeling (Hawaii)
R. Glenn Morris (KIPAC)
Andy Fabian (Cambridge)

(+ D. Applegate, M. Bradac,
P. Burchat, D. Burke, E. Million,
L. Wilden + ...)

Cluster cosmology: a proud history

Galaxy clusters are the largest objects in the Universe (10^{14} – few 10^{15} Msun) and have a long history as powerful cosmological probes.



Discovery of
Dark Matter

(Zwicky 1933)

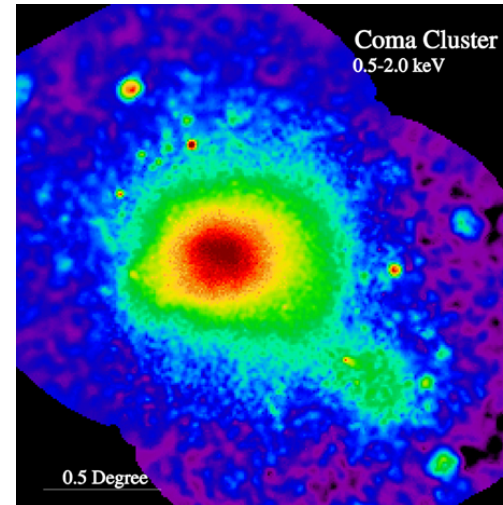
Coma Cluster
(optical light)

Application of virial theorem to galaxy motions \rightarrow ~ 100 times more mass than expected by adding up all of the mass in stars.

X-ray cluster cosmology: major contributions

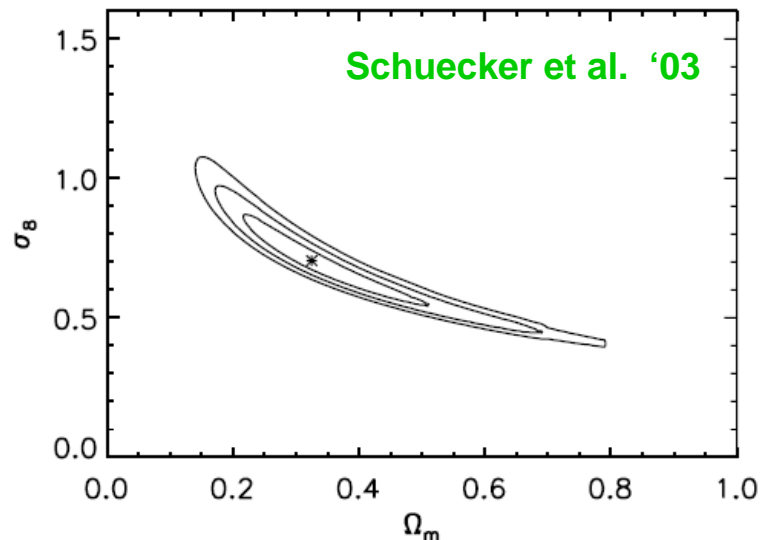
First to show $\Omega_m \sim 0.3$

Based on observed baryonic mass fraction in clusters (White et al. '93 and many papers thereafter).



First to show $\sigma_8 \sim 0.75$

Based on observed X-ray number counts of clusters (eg Borgani et al. '01, Seljak '02; Allen et al. '03; Pierpaoli et al. '03 Schuecker et al '03)



The separation of dark and normal matter in clusters

The combination of X-ray and gravitational lensing data for the 'bullet cluster' 1E0657-56 (a merger of two large clusters) confirms that dark matter is very different in nature from the bulk of normal, baryonic matter (X-ray emitting gas).



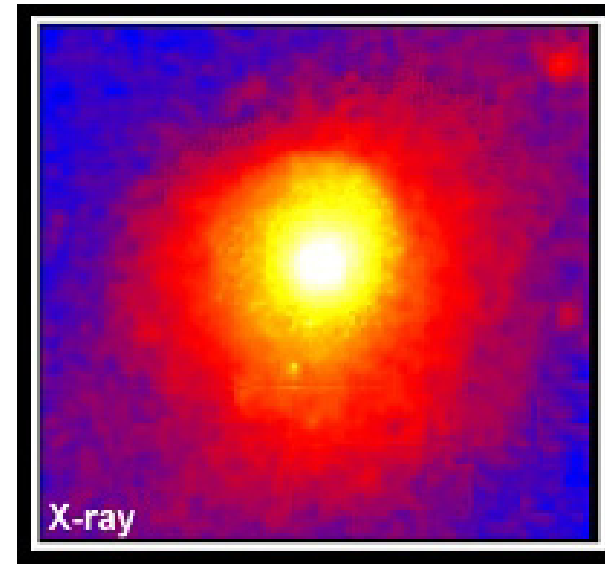
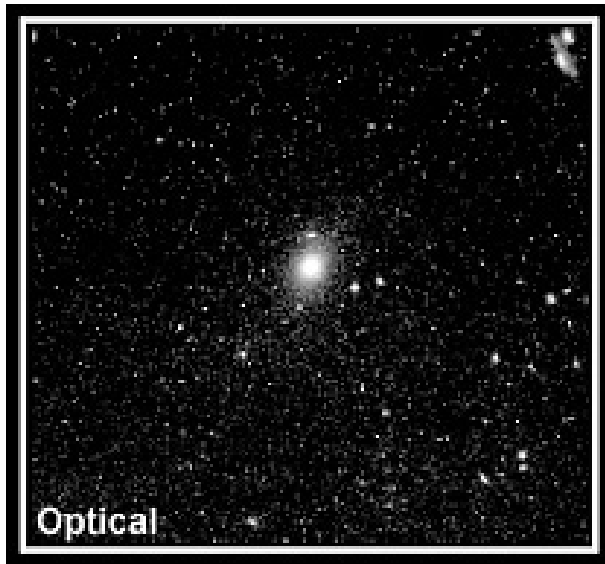
X-ray emitting gas
feels ram pressure
whereas dark matter
(and galaxies) pass
through (at least
relatively) unhindered.

**Consistent with weakly
interacting, cold dark
matter (CDM) paradigm.**

Markevitch et al. '04
Clowe et al '04, '07
Bradac et al. '07

Why study clusters at X-ray wavelengths?

Most baryons in clusters (like Universe) are in form of gas, not stars (6x more).
In clusters, gravity squeezes gas, heating it to X-ray temperatures (10^7 - 10^8 K)

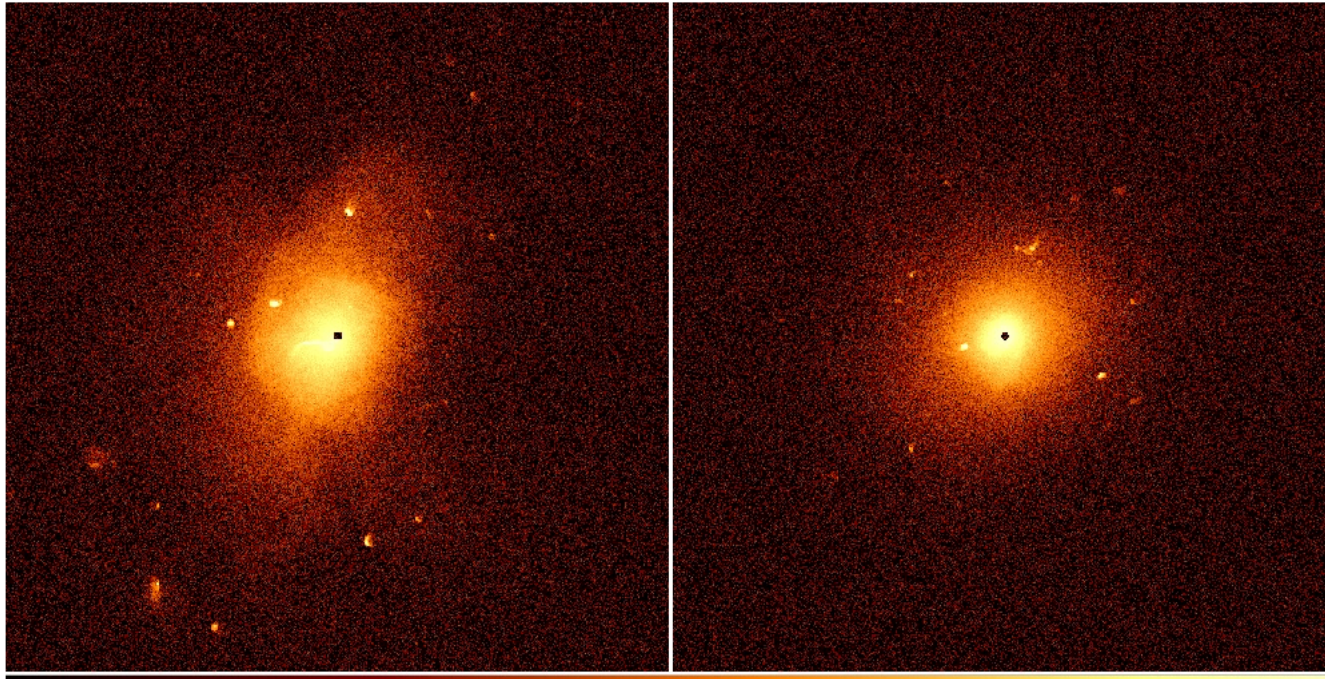


Since clusters only shine in X-rays if they really are massive, X-ray observations produce remarkably [clean cluster catalogues](#), vital for cosmology.

Primary X-ray observables (density, temperature) relate directly to total (dark plus luminous) mass in a way that's well understood (hydrostatic equilibrium) and can be well modelled by hydro. simulations.

Hydro simulations of X-ray clusters

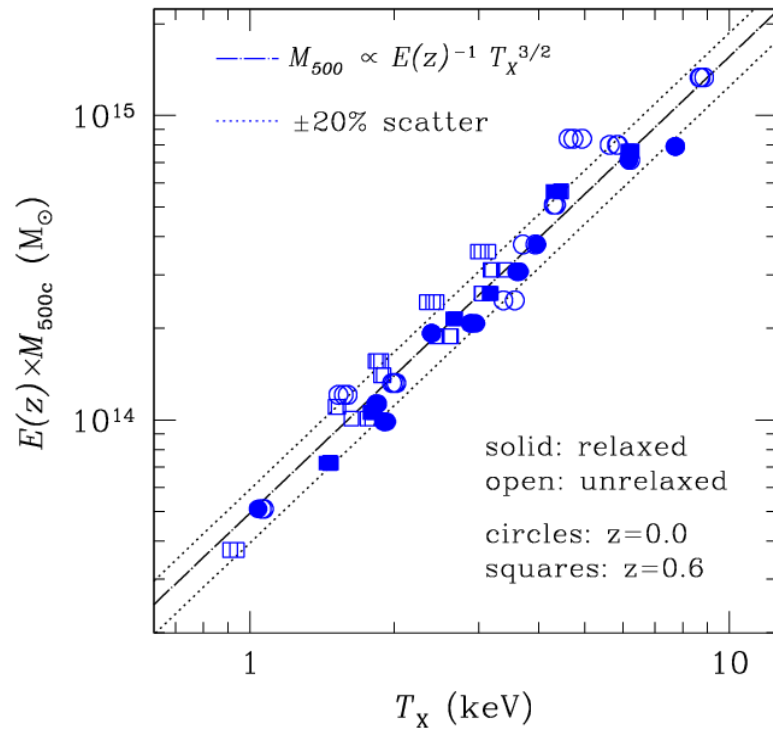
Nagai, Vikhlinin & Kravtsov '07



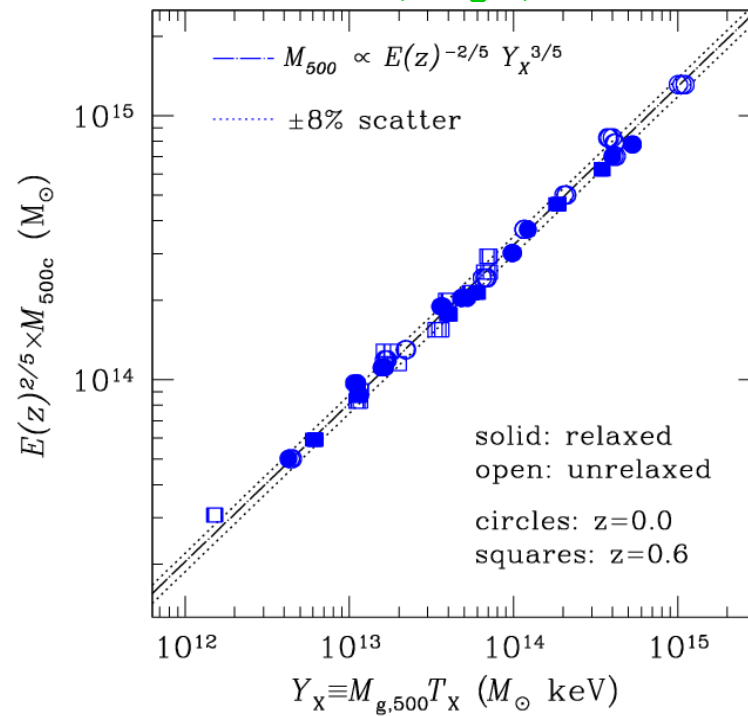
Large, independent programs have been undertaken to simulate X-ray observations of clusters using state-of-the-art hydro codes and selecting/analysing these systems in an identical manner to real observations.

The most recent results have provided very good news for X-ray cluster cosmology: systematics are relatively small and can be quantified.

X-ray observables correlate tightly with mass



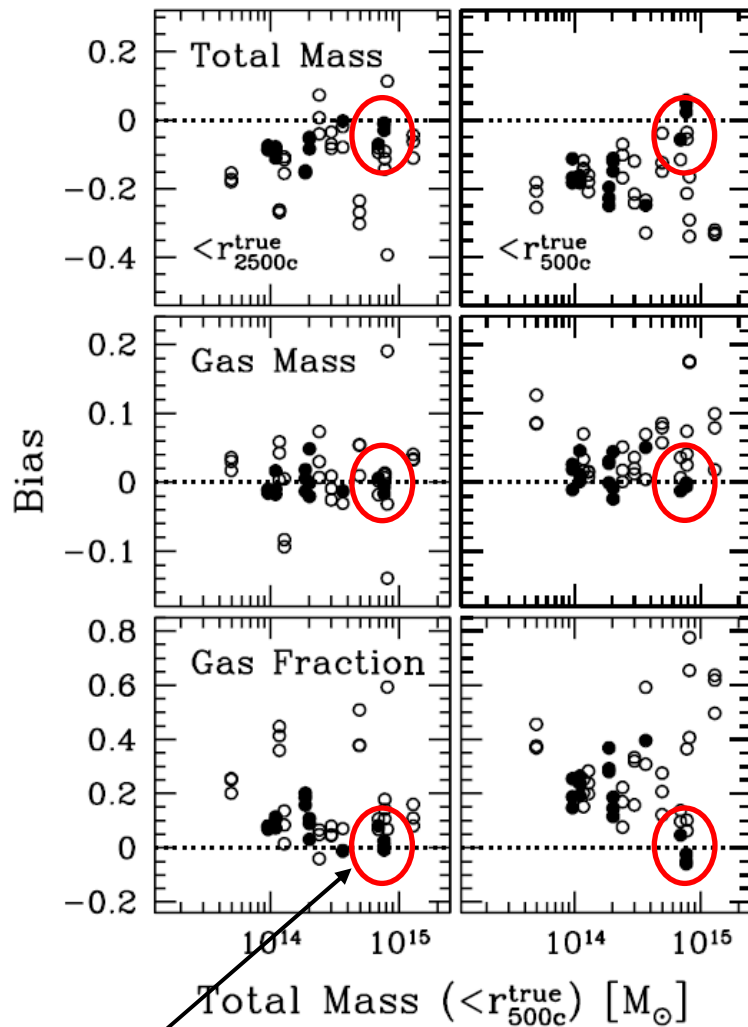
Kravtsov, Nagai, Vikhlinin '06



- The correlations are tight and independent of the background cosmology.
- The scatter between the observables and total mass is LOW.

For relaxed clusters, X-ray studies → precise masses

Nagai, Vikhlinin & Kravtsov '07



Relaxed clusters (filled circles)

For largest, relaxed clusters (selected on X-ray morphology) we expect to measure (w/ current technology)

X-ray gas mass to ~1% accuracy.

Total mass to several % accuracy (both bias and scatter).

Primary uncertainty (beyond innermost core) is residual bulk motions in gas. (High spectral resolution X-ray maps required to measure gas velocities.)

Bottom line:

X-ray studies of relaxed clusters allow precise, robust measurements of the distributions of both baryonic and dark matter → crucial for cosmology

Outline of the talk

1) Testing the cold dark matter (CDM) paradigm in relaxed clusters

Compare the observed mass profiles and concentration-mass relation for the largest, relaxed X-ray luminous galaxy clusters with the predictions from CDM cosmological simulations.

2) Constraints on cosmology from X-ray studies of galaxy clusters

Constraints on the mean matter density Ω_m and dark energy ($\Omega_{de,w}$) from measurements of the baryonic mass fraction in the largest relaxed clusters (absolute distance measurements).

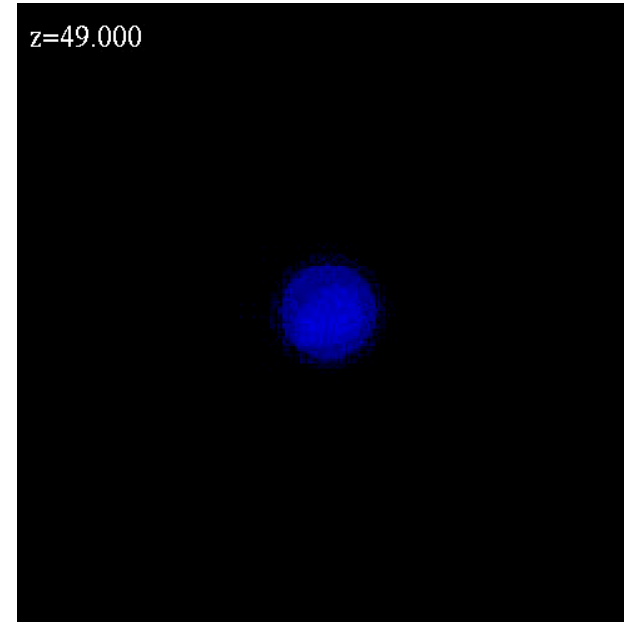
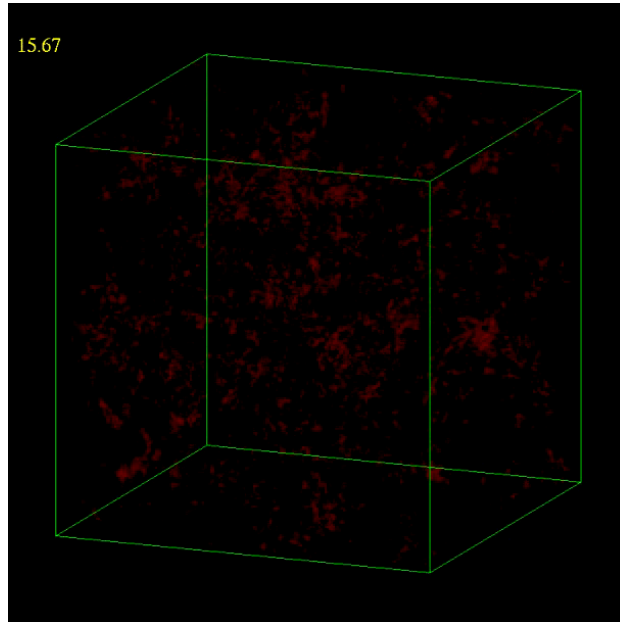
Constraints on the mean matter density Ω_m , the amplitude of matter fluctuations σ_8 , and dark energy ($\Omega_{de,w}$), from the evolution of the number density of X-ray luminous clusters (growth of cosmic structure).

1: Testing the CDM paradigm

The dark matter halos of massive, relaxed galaxy clusters

Schmidt & Allen 2007, MNRAS 379, 209 (astro-ph/0610038)

Predictions for relaxed CDM halos from simulations



B. Moore et al.

1) A 'Universal' CDM density profile

$$\rho(r) = \frac{\rho_0}{\left(\frac{r}{r_s}\right)^\alpha \left(1 + \frac{r}{r_s}\right)^{3-\alpha}}$$

eg Navarro, Frenk & White '95, '97,
Moore et al. '99, Diemand et al. '04.
Inner dark matter density slope $\alpha \sim 1$.

2) A tight relation between halo concentration ($c=r_{\text{vir}}/r_s$) and mass: lower mass halos form earlier and are more concentrated.

The Chandra X-ray Observatory



Launched July 1999. One of NASA's four Great Observatories (HST, CGRO, Spitzer).

Instruments:

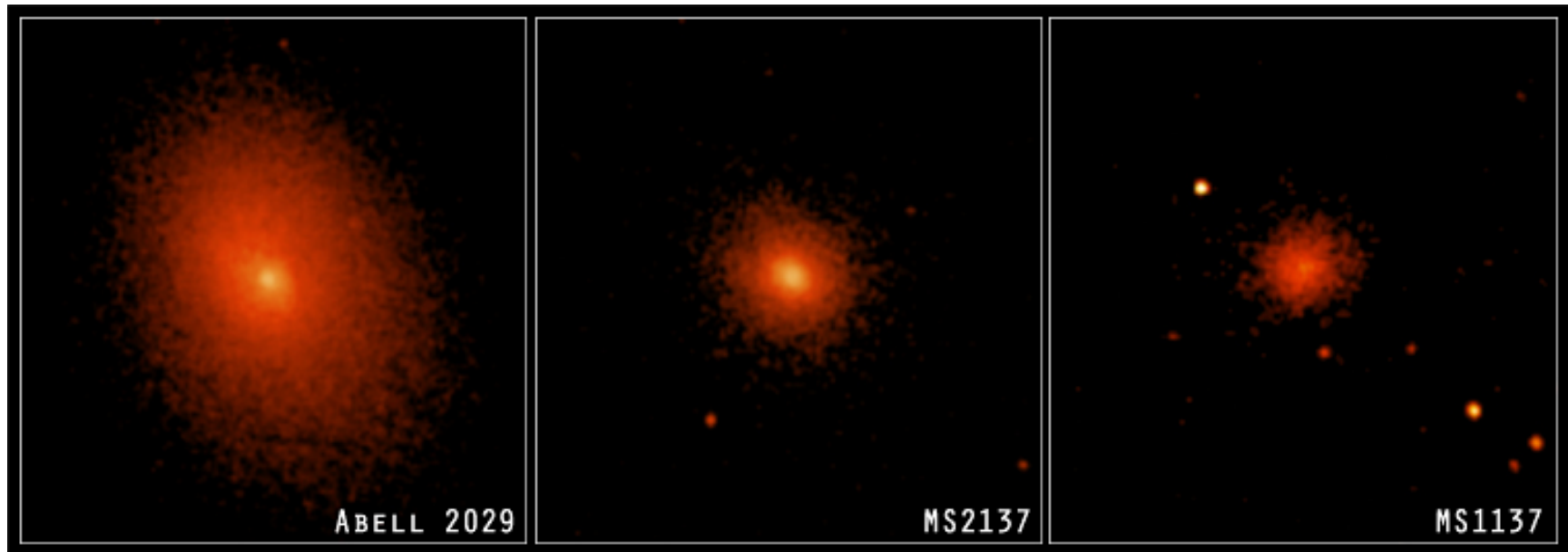
Micro-channel plate detector (HRC)
Transmission gratings (LETG/HETG)
Advanced CCD Imaging Spectrometer

ACIS main features: Charged Coupled Device array (X-ray CCDs).
Field of view 16×16 arcmin² (ACIS-I). Good spectral resolution ~ 100 eV over 0.5-8 keV range. Exquisite spatial resolution (0.5 arcsec FWHM).

Chandra and (XMM-Newton) provided first opportunity to carry out detailed spatially-resolved X-ray spectroscopy of galaxy clusters

→ revolutionized cosmological work.

The Chandra data



34 hot ($kT > 5\text{keV}$), highly X-ray luminous ($L_x > 10^{45} h_{70}^{-2} \text{ erg/s}$), dynamically relaxed clusters spanning redshifts $0 < z < 0.7$ (lookback time of 6Gyr)

Regular X-ray morphology: sharp central X-ray surface brightness peak, minimal X-ray isophote centroid variation, low power-ratios (morphological selection).

(These systems are very different from the bullet cluster!)

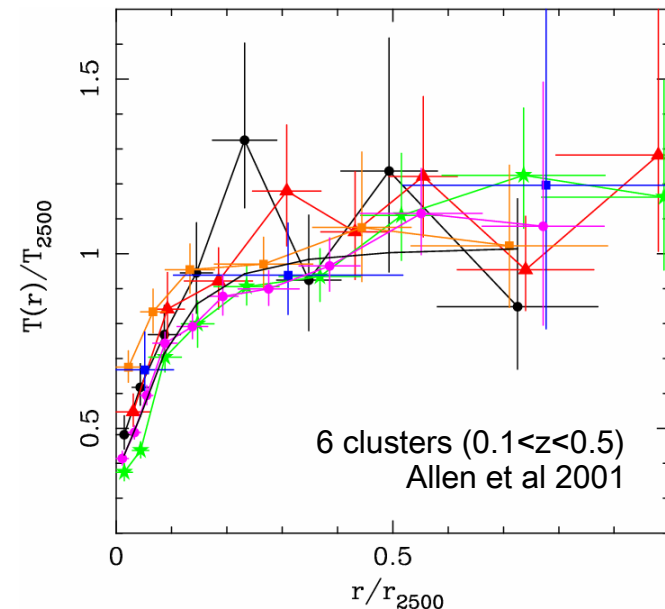
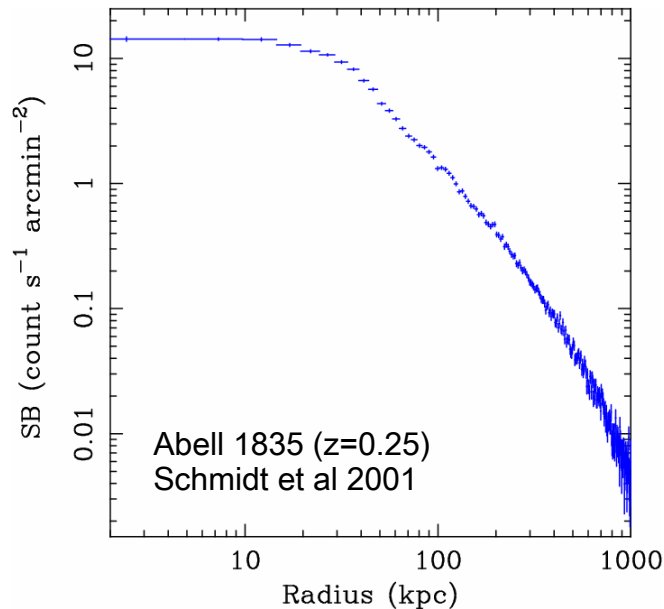
X-ray mass measurements

- Observables:**
- 1) observed X-ray surface brightness (SB) profile.
 - 2) deprojected (spectrally-determined) temperature (kT) profile.

→ X-ray gas density profile

+ assumption of hydrostatic equilibrium (symmetry) → **total mass, $M_{\text{tot}}(r)$.**

$$M_{\text{tot}}(r) = -\frac{rkT}{G\mu m_p} \left(\frac{d \ln n_e}{d \ln r} + \frac{d \ln T}{d \ln r} \right)$$



X-ray mass measurements

For accurate, precise mass measurements:

1) Should NOT assume isothermality.

2) If using simple parameterizations to fit SB, kT profiles, make sure these models provide acceptable fits and remember that they bring strong priors into the analysis (which can complicate the interpretation of results).

Our approach uses a minimum of priors (neither of the above):

Take a parameterized (total) mass model + SB profile (+ assumption that pressure has smooth power law form at outer edge of cluster) ...

e.g. NFW profile
(Free params c, r_s)

$$\rho(r) = \frac{\rho_0}{\left(\frac{r}{r_s}\right)\left(1 + \frac{r}{r_s}\right)^2}$$

... and, for a given set of parameters:

Use MC simulations to predict kT(r) → compare with obs.

→ does model provide acceptable fit?

→ best-fit params and confidence limits

The total mass (dark+luminous matter) profiles

Question 1: Does the NFW model provide a statistically acceptable description of the total mass (dark+luminous matter) profiles in the clusters?

$$\rho(r) = \frac{\rho_0}{\left(\frac{r}{r_s}\right)\left(1 + \frac{r}{r_s}\right)^2}$$

Result 1: **YES!** The NFW provides a good description of the data (32/34).

Question 2: Can a singular, isothermal (SI) density profile provide a statistically acceptable description of the total mass profiles in the clusters?

$$\rho(r) = A/r^2$$

Result 2: **NO!** The SI model is completely rejected in almost every case (32/34)

Summary of results on the total mass profiles

TOTAL MASS (LUMINOUS PLUS DARK MATTER)					
Number of kT bins	NFW MODEL			SI MODEL	
	r_s	c	χ^2/DOF	χ^2/DOF	
Abell 1795	5	0.41 ^{+0.14} _{-0.07}	4.62 ^{+0.65} _{-0.79}	1.67/3	49.2/4
Abell 2029	6	0.27 ^{+0.05} _{-0.02}	7.06 ^{+0.26} _{-0.74}	4.94/4	303/5
Abell 478	7	0.50 ^{+0.06} _{-0.07}	4.47 ^{+0.45} _{-0.28}	8.88/5	615/6
PKS0745-191	7	0.35 ^{+0.13} _{-0.09}	6.24 ^{+1.38} _{-1.10}	5.17/5	42.1/6
Abell 1413	6	0.51 ^{+0.11} _{-0.09}	4.18 ^{+0.83} _{-0.51}	24.6/5	91.5/6
Abell 2204	5	0.19 ^{+0.09} _{-0.05}	9.74 ^{+0.12} _{-2.25}	4.41/3	16.6/4
Abell 383	5	0.48 ^{+0.12} _{-0.12}	3.75 ^{+0.71} _{-0.48}	23.3/4	90.0/5
Abell 963	5	0.40 ^{+0.12} _{-0.11}	4.61 ^{+1.07} _{-0.73}	6.19/3	97.8/4
RXJ0439.0+0521	4	0.19 ^{+0.06} _{-0.05}	7.69 ^{+1.52} _{-1.29}	0.30/2	28.3/3
RXJ1504.1-0248	5	0.54 ^{+0.29} _{-0.15}	4.38 ^{+1.06} _{-1.05}	0.91/3	28.1/4
RXJ2129.6+0005	5	0.38 ^{+0.45} _{-0.17}	4.59 ^{+2.18} _{-1.84}	1.53/3	14.7/4
Abell 1835	5	0.58 ^{+0.08} _{-0.10}	4.20 ^{+0.52} _{-0.31}	12.5/3	302/4
Abell 611	5	0.33 ^{+0.19} _{-0.12}	5.32 ^{+1.86} _{-1.49}	2.35/3	25.7/4
Zwicky 3146	5	0.99 ^{+>5.0} _{-0.58}	2.71 ^{+2.38} _{-2.71}	0.79/3	11.4/4
Abell 2537	5	0.36 ^{+0.37} _{-0.12}	4.97 ^{+1.52} _{-1.87}	3.30/3	22.2/4
MS2137.3-2353	6	0.18 ^{+0.02} _{-0.02}	8.08 ^{+0.81} _{-0.45}	5.55/4	235/5
MACSJ0242.6-2132	4	0.18 ^{+0.02} _{-0.01}	7.97 ^{+0.85} _{-1.12}	2.93/2	62.1/3
MACSJ1427.6-2521	4	0.16 ^{+0.06} _{-0.06}	8.08 ^{+2.62} _{-1.87}	4.78/2	18.1/3
MACSJ2229.8-2756	4	0.15 ^{+0.10} _{-0.05}	8.43 ^{+3.20} _{-2.55}	1.60/2	6.8/3
MACSJ0947.2+7623	4	0.31 ^{+0.19} _{-0.10}	6.15 ^{+1.75} _{-1.58}	2.56/2	23.6/3
MACSJ1931.8-2635	4	0.51 ^{+0.94} _{-0.19}	4.05 ^{+1.42} _{-1.91}	1.98/2	33.6/3
MACSJ1115.8+0129	4	1.35 ^{+>5.0} _{-0.91}	2.15 ^{+2.20} _{-2.15}	1.24/2	13.7/3
MACSJ1532.9+3021	5	0.33 ^{+0.17} _{-0.08}	5.36 ^{+1.18} _{-1.19}	1.77/3	41.8/4
MACSJ0011.7-1523	4	0.49 ^{+0.16} _{-0.14}	3.75 ^{+0.83} _{-0.62}	6.75/2	168/3
MACSJ1720.3+3536	4	0.33 ^{+0.14} _{-0.08}	5.21 ^{+0.98} _{-1.00}	1.19/2	49.8/3
MACSJ0429.6-0253	4	0.16 ^{+0.04} _{-0.04}	8.46 ^{+1.32} _{-1.07}	1.87/2	25.8/3
MACSJ0159.8-0849	4	0.35 ^{+0.12} _{-0.08}	5.49 ^{+0.97} _{-0.86}	4.45/2	52.9/3
MACSJ0329.7-0212	4	0.29 ^{+0.07} _{-0.05}	5.48 ^{+0.62} _{-0.62}	6.24/2	86.0/3
RXJ1347.5-1144	6	0.45 ^{+0.11} _{-0.07}	5.63 ^{+0.64} _{-0.67}	16.1/4	257/5
3C295	4	0.15 ^{+0.02} _{-0.03}	8.64 ^{+1.05} _{-0.85}	1.12/2	61.3/3
MACSJ1621.6+3810	4	0.25 ^{+0.18} _{-0.10}	6.51 ^{+2.57} _{-2.04}	4.01/2	17.6/3
MACSJ1311.0-0311	4	0.31 ^{+0.15} _{-0.09}	4.91 ^{+1.28} _{-1.10}	1.55/2	25.4/3
MACSJ1423.8+2404	4	0.17 ^{+0.03} _{-0.02}	8.27 ^{+0.89} _{-0.74}	0.07/2	74.1/3
MACSJ0744.9+3927	4	0.32 ^{+0.19} _{-0.08}	4.88 ^{+1.03} _{-1.30}	4.40/2	40.9/3

Result 1:

The NFW model provides an acceptable description of the total mass profiles in ~32/34 clusters

Result 2:

The singular isothermal model can be rejected in almost every case.

The dark matter profiles

The X-ray data can also be used to recover the dark matter profiles in the clusters if the distribution of baryonic matter is known.

- 1) The X-ray emitting gas density profile can be determined from the X-ray surface brightness and gas temperature to high accuracy.
- 2) The stellar mass profile can be obtained from optical/IR data. Small o/a contribution to total mass ($\sim 2\%$) but important to model cD galaxy appropriately. Systematic uncertainties relatively small.

Plug in the X-ray emitting gas and stellar mass profiles; let the dark matter be modelled with an NFW profile, as before.

For a given set of parameters:

Let the total mass be the sum of the dark matter plus the above baryonic matter components and, as before:

Use MC simulations to predict $kT(r)$ → compare with obs.
→ **best-fit params and confidence limits**

The dark matter profiles

Question 3: Does the NFW model provide a statistically acceptable description of the dark matter profiles in the clusters?

$$\rho(r) = \frac{\rho_0}{\left(\frac{r}{r_s}\right)\left(1 + \frac{r}{r_s}\right)^2}$$

Result 3: **YES!** The NFW provides a good description of the dark matter profiles in 32/34 clusters.

The dark matter profiles

Question 4: How does the measured inner dark matter density slope compare with the prediction from CDM simulations: $\alpha \sim 1 (\pm 0.4)$?

Method: replace the NFW model with a more general profile in which the inner dark matter density slope is a free parameter and repeat analysis.

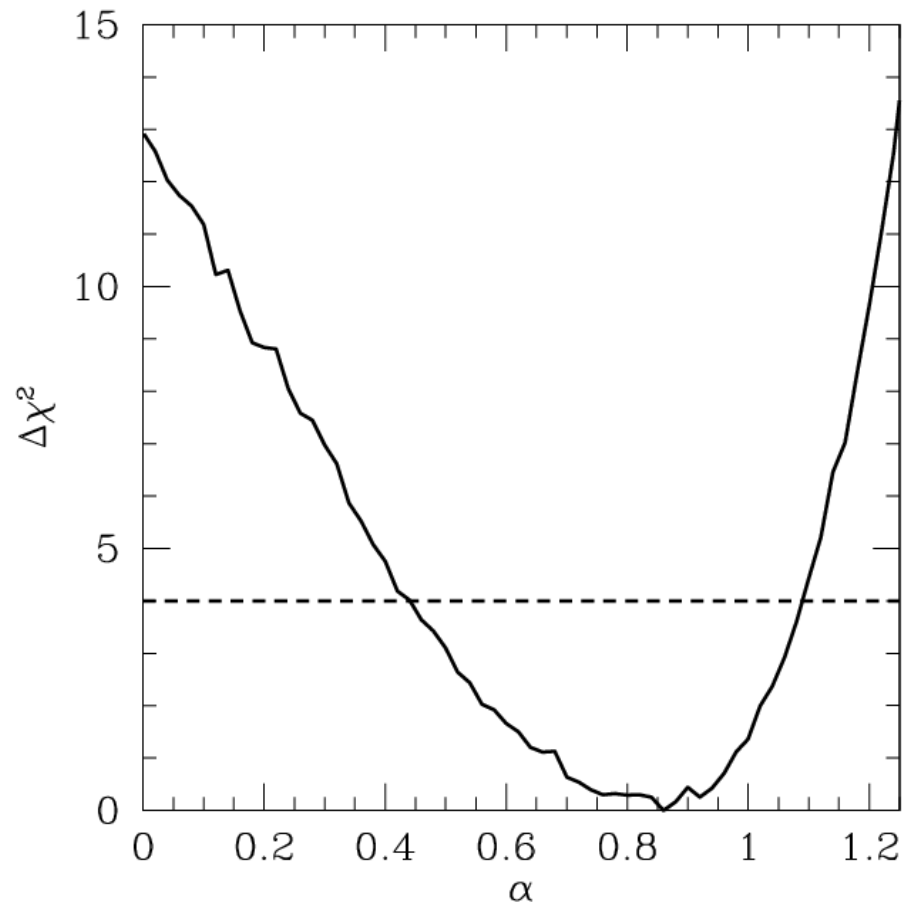
$$\rho(r) = \frac{\rho_0}{\left(\frac{r}{r_s}\right)^\alpha \left(1 + \frac{r}{r_s}\right)^{3-\alpha}} \quad \text{'Generalized NFW model'}$$

Result 4a: 80% of observed profiles have inner slope consistent with unity at 68% confidence.

Combining the results for all clusters for which the generalized NFW model provides an acceptable fit we obtain the following....

The dark matter profiles

Result 5b: Combined constraint on the inner DM density profile



$\alpha=0.88$ (+0.26, -0.31)
95% confidence limits.

**Combined result on inner DM
density slope consistent with
CDM predictions ($\alpha \sim 1$).**

Summary of results on the dark matter profiles

	DARK MATTER PROFILES				
	NFW ($\alpha = 1$)			GENERALIZED NFW	
	r_s	c	χ^2/DOF	α	χ^2/DOF
Abell 1795	0.47 ^{+0.12} _{-0.13}	4.02 ^{+1.03} _{-0.57}	1.90/3	0.00 ^{+1.29}	1.35/2
Abell 2029	0.29 ^{+0.02} _{-0.03}	6.41 ^{+0.47} _{-0.30}	4.34/4	1.00 ^{+0.35} _{-0.31}	4.14/3
Abell 478	0.60 ^{+0.10} _{-0.08}	3.72 ^{+0.35} _{-0.33}	6.81/5	1.06 ^{+0.12} _{-0.26}	6.68/4
PKS0745-191	0.36 ^{+0.14} _{-0.10}	5.80 ^{+1.49} _{-1.10}	5.30/5	0.70 ^{+0.71}	5.19/4
Abell 1413	0.50 ^{+0.11} _{-0.11}	4.21 ^{+0.46} _{-0.49}	24.5/5	1.54 ^{+0.06} _{-0.21}	22.0/4
Abell 2204	0.20 ^{+0.07} _{-0.07}	9.28 ^{+3.32} _{-1.80}	5.05/3	0.00 ^{+0.88}	3.69/2
Abell 383	0.46 ^{+0.17} _{-0.10}	3.70 ^{+0.65} _{-0.67}	23.6/3	0.00 ^{+0.40}	20.1/2
Abell 963	0.43 ^{+0.16} _{-0.13}	4.13 ^{+0.95} _{-0.78}	7.59/3	0.00 ^{+0.54}	4.84/2
RXJ0439.0+0521	0.22 ^{+0.09} _{-0.06}	6.41 ^{+1.38} _{-1.25}	0.73/2	0.00 ^{+1.16}	0.08/1
RXJ1504.1-0248	0.65 ^{+0.41} _{-0.22}	3.62 ^{+1.14} _{-0.97}	0.85/3	0.94 ^{+0.59}	0.85/2
RXJ2129.6+0005	0.41 ^{+0.86} _{-0.20}	3.99 ^{+2.15} _{-2.06}	1.53/3	1.00 ^{+0.58}	1.52/2
Abell 1835	0.74 ^{+0.19} _{-0.14}	3.31 ^{+0.42} _{-0.42}	14.9/3	0.00 ^{+0.69}	11.4/2
Abell 611	0.33 ^{+0.27} _{-0.11}	5.02 ^{+1.64} _{-1.69}	2.47/3	0.52 ^{+1.04}	2.38/2
Zwicky 3146	1.14 ^{+>5.0} _{-0.71}	2.31 ^{+2.27} _{-2.31}	0.84/3	0.00 ^{+1.51}	0.64/2
Abell 2537	0.42 ^{+0.44} _{-0.18}	4.31 ^{+2.04} _{-1.65}	3.70/3	0.00 ^{+0.89}	2.51/2
MS2137.3-2353	0.21 ^{+0.03} _{-0.02}	6.95 ^{+0.55} _{-0.60}	5.22/4	0.92 ^{+0.28} _{-0.40}	5.18/3
MACSJ0242.6-2132	0.23 ^{+0.07} _{-0.05}	6.46 ^{+1.12} _{-0.99}	3.07/2	0.60 ^{+0.66}	2.83/1
MACSJ1427.6-2521	0.19 ^{+0.14} _{-0.07}	6.71 ^{+2.24} _{-1.98}	4.99/2	0.00 ^{+1.57}	4.71/1
MACSJ2229.8-2756	0.17 ^{+0.13} _{-0.07}	7.27 ^{+3.82} _{-2.38}	1.47/2	1.66 ^{+0.16}	1.04/1
MACSJ0947.2+7623	0.37 ^{+0.24} _{-0.15}	5.17 ^{+1.98} _{-1.38}	2.70/2	0.00 ^{+1.18}	2.06/1
MACSJ1931.8-2635	0.70 ^{+3.06} _{-0.35}	3.07 ^{+1.81} _{-1.98}	1.84/2	1.16 ^{+0.35}	1.82/1
MACSJ1115.8+0129	1.64 ^{+>5.0} _{-1.16}	1.77 ^{+2.11} _{-1.77}	1.33/2	0.00 ^{+1.35}	1.05/1
MACSJ1532.9+3021	0.37 ^{+0.25} _{-0.11}	4.66 ^{+1.25} _{-1.30}	2.14/3	0.00 ^{+1.16}	1.45/2
MACSJ0011.7-1523	0.63 ^{+0.31} _{-0.21}	2.94 ^{+0.85} _{-0.65}	8.93/2	0.00 ^{+0.40}	5.02/1
MACSJ1720.3+3536	0.44 ^{+0.19} _{-0.16}	4.04 ^{+1.29} _{-0.80}	1.14/2	1.12 ^{+0.32}	1.12/1
MACSJ0429.6-0253	0.17 ^{+0.06} _{-0.04}	7.51 ^{+1.36} _{-1.26}	1.30/2	1.38 ^{+0.28} _{-0.69}	0.78/1
MACSJ0159.8-0849	0.41 ^{+0.19} _{-0.12}	4.64 ^{+1.09} _{-0.96}	3.43/2	1.42 ^{+0.08} _{-0.22}	1.51/1
MACSJ0329.7-0212	0.34 ^{+0.12} _{-0.08}	4.51 ^{+0.76} _{-0.75}	7.10/2	0.00 ^{+0.81}	5.56/1
RXJ1347.5-1144	0.55 ^{+0.10} _{-0.11}	4.72 ^{+0.61} _{-0.45}	18.9/4	0.00 ^{+0.35}	10.3/3
3C295	0.17 ^{+0.04} _{-0.03}	7.49 ^{+0.97} _{-0.86}	1.89/2	0.00 ^{+0.99}	0.86/1
MACSJ1621.6+3810	0.27 ^{+0.22} _{-0.11}	5.85 ^{+2.78} _{-1.93}	4.13/2	0.00 ^{+1.59}	3.98/1
MACSJ1311.0-0311	0.35 ^{+0.19} _{-0.13}	4.24 ^{+1.40} _{-1.00}	1.42/2	1.46 ^{+0.12} _{-1.14}	0.92/1
MACSJ1423.8+2404	0.18 ^{+0.04} _{-0.02}	7.55 ^{+0.63} _{-0.87}	0.29/2	0.62 ^{+0.63}	0.02/1
MACSJ0744.9+3927	0.37 ^{+0.23} _{-0.13}	4.21 ^{+1.39} _{-1.07}	4.87/2	0.00 ^{+0.78}	3.32/1

Result 3:

The NFW model provides an acceptable description of the dark matter profiles in ~32/34 clusters

Result 4:

The inner dark matter density slope is consistent with the CDM prediction of $\alpha \sim 1$.

The concentration-mass (c - M_{vir}) relation

Question 5: How does the observed concentration-mass relation compare to the predictions from numerical simulations?

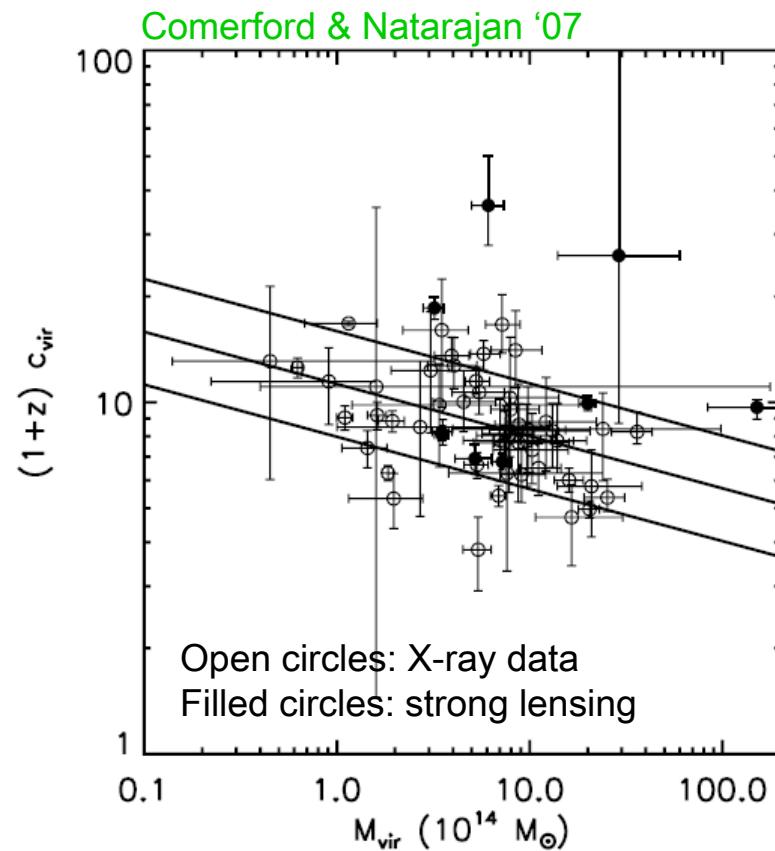
Generic CDM model predictions:

- 1) Smaller mass halos are more concentrated than larger ones.
- 2) Slope of c - M relation: at fixed z , $c \propto M_{\text{vir}}^a$ with $a \approx -0.1$.
- 3) Evolution: at fixed M_{vir} , c evolves approximately as $1/(1+z)$.
- 4) Intrinsic dispersion at fixed mass $\Delta \log c \sim 0.1$.

(see R. Wechsler talk)

The concentration-mass (c - M_{vir}) relation

Result 5: The observed c - M_{vir} relation is in good, overall agreement with the predictions from simulations



Slope, scatter and evolution consistent with predictions. Normalization slightly higher than CDM-only predictions. However, correctly modelling the effects of baryons may account for this (e.g. Rudd et al '07; R. Wechsler talk).

Data: Schmidt & Allen '07,
Buote et al. '07,
Comerford & Natarajan '07.

Overall conclusion from Part 1:

The cold dark matter (CDM) paradigm holds up very well under scrutiny from Chandra X-ray observations of relaxed galaxy clusters.

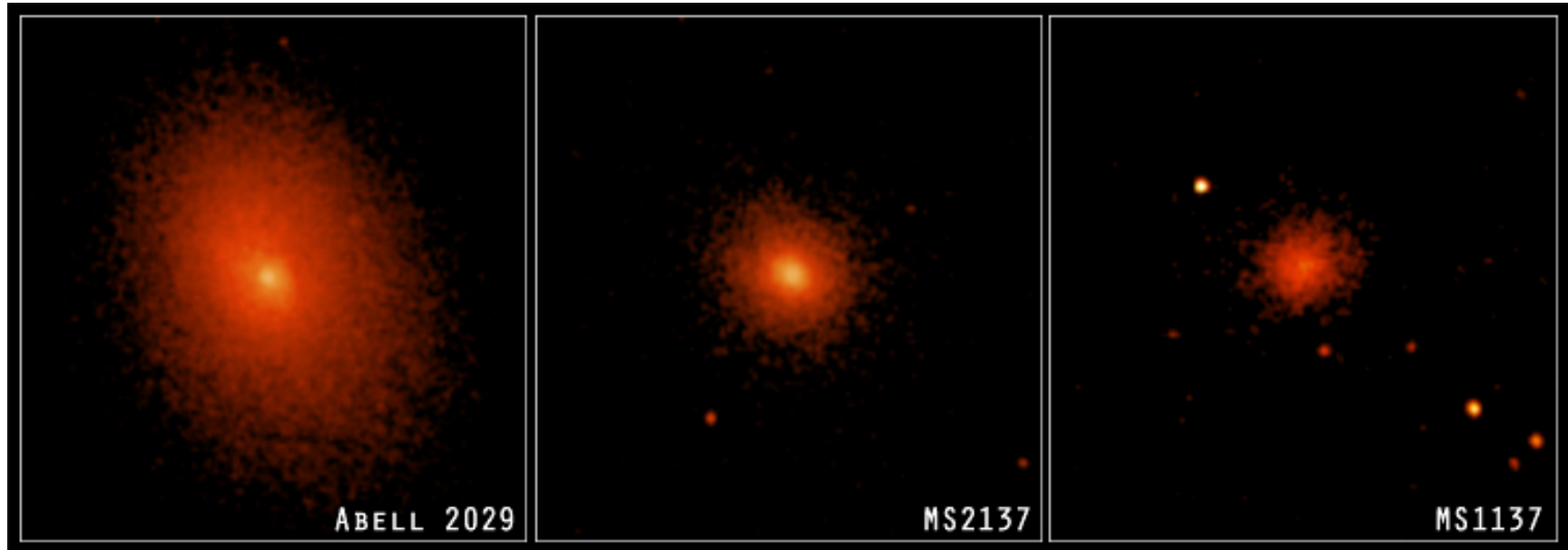
Mass profiles of relaxed clusters are consistent with CDM predictions.

Probing cosmology with X-ray clusters

2a: Absolute distance measurements (the fgas experiment)

Allen et al 2007, MNRAS, submitted (astro-ph/0706.0033)

The Chandra data



42 hot ($kT > 5\text{keV}$), highly X-ray luminous ($L_x > 10^{45} h_{70}^{-2} \text{ erg/s}$), dynamically relaxed clusters spanning redshifts $0 < z < 1.1$ (lookback time of 8Gyr)

Regular X-ray morphology: sharp central X-ray surface brightness peak, minimal X-ray isophote centroid variation, low power-ratios (morphological selection).

Constraining Ω_m with f_{gas} measurements

BASIC IDEA (White & Frenk 1991): Galaxy clusters are so large that their matter content should provide a fair sample of matter content of Universe.

For relaxed clusters: X-ray data \rightarrow precise total mass measurements
 \rightarrow very precise X-ray gas mass measurements

If we define:

$$f_{\text{gas}} = \frac{\text{X-ray gas mass}}{\text{total cluster mass}} \quad s = f_{\text{star}}/f_{\text{gas}} \sim 0.16$$

eg Lin & Mohr 04
Fukugita et al '98

Then:

$$f_{\text{baryon}} = f_{\text{star}} + f_{\text{gas}} = f_{\text{gas}}(1 + s)$$

Since clusters provide \sim fair sample of Universe $f_{\text{baryon}} = b\Omega_b/\Omega_m$

$$\Omega_m = \frac{b\Omega_b}{f_{\text{baryon}}} = \frac{b\Omega_b}{f_{\text{gas}}(1+s)}$$

The depletion factor, b

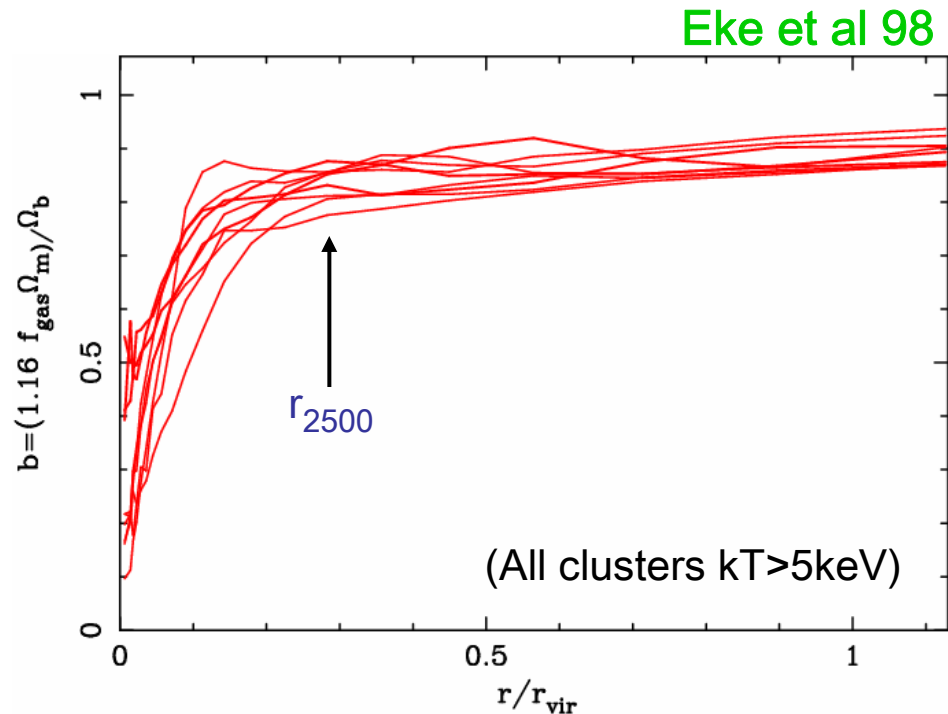
Simulations:

$$f_{\text{baryon}} = b \frac{\Omega_b}{\Omega_m}$$

For $r \sim 0.25 r_{\text{vir}}$ (Chandra obs.)

$$b = 0.83 \pm 0.09$$

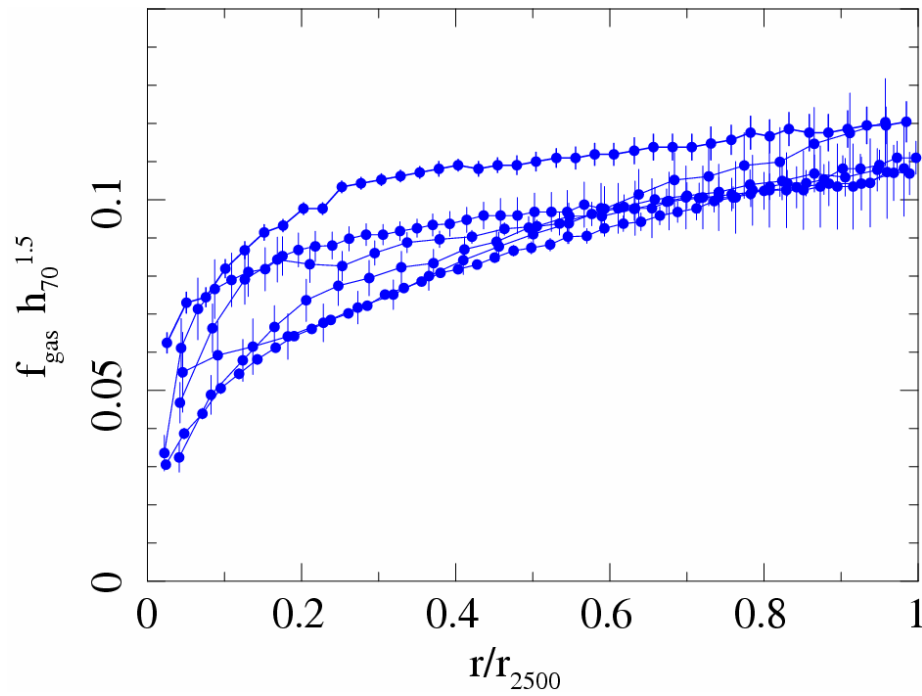
(non-radiative simulations +
10% systematic uncertainty)



Simulations indicate that baryonic mass fraction in clusters is slightly lower than mean value for Universe as a whole. (Some gas is lifted beyond the virial radius by shocks e.g. Evrard '90, Thomas & Couchman '92, Navarro & White '93; NFW '95 etc)

See also e.g. Crain et al. '07 (astro-ph/0610602).

Chandra results on $f_{\text{gas}}(r)$



6 lowest redshift relaxed clusters ($0 < z < 0.15$) :

$f_{\text{gas}}(r) \rightarrow$ approximately universal value at r_{2500}

Fit constant value at r_{2500}

$$f_{\text{gas}}(r_{2500}) = (0.113 \pm 0.003) h_{70}^{-1.5}$$

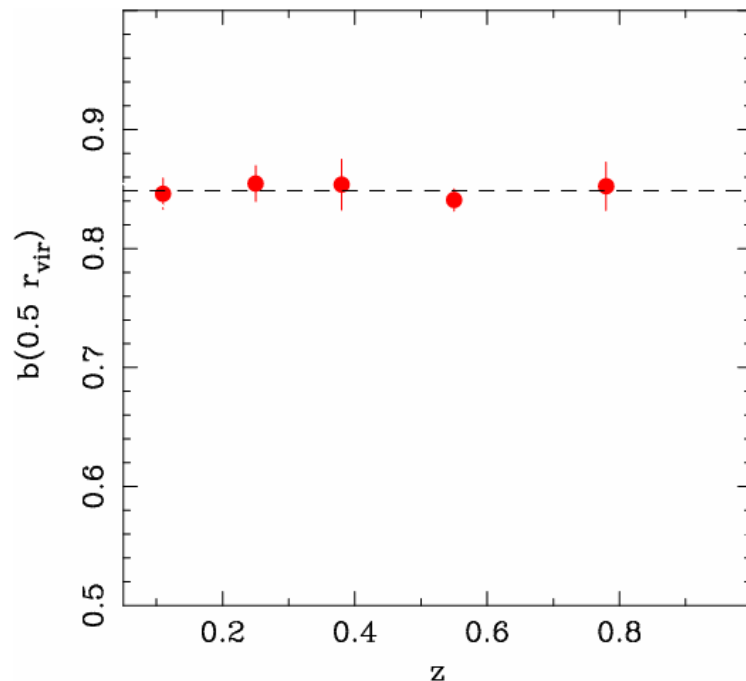
For $\Omega_b h^2 = 0.0214 \pm 0.0020$ (Kirkman et al. '03), $h = 0.72 \pm 0.08$ (Freedman et al. '01), $b = 0.83 \pm 0.09$ (Eke et al. 98 +10% allowance for systematics in calibration/modelling)

$$\Omega_m = \frac{(0.83 \pm 0.09)(0.0437 \pm 0.0041)h_{70}^{-0.5}}{(0.113 \pm 0.003)(1 + [0.16 \pm 0.05]h_{70}^{0.5})} = 0.27 \pm 0.04$$

Constraining dark energy with f_{gas} measurements

The measured f_{gas} values depend upon assumed distances to clusters $f_{\text{gas}} \propto d^{1.5}$. This introduces apparent systematic variations in $f_{\text{gas}}(z)$ depending on differences between reference cosmology and true cosmology.

What do we expect to observe?



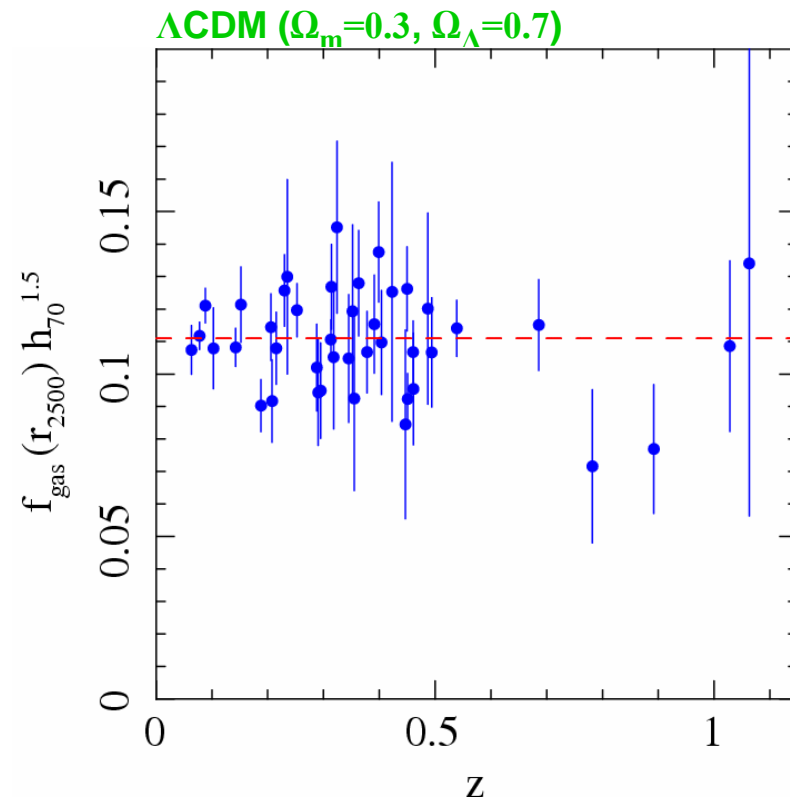
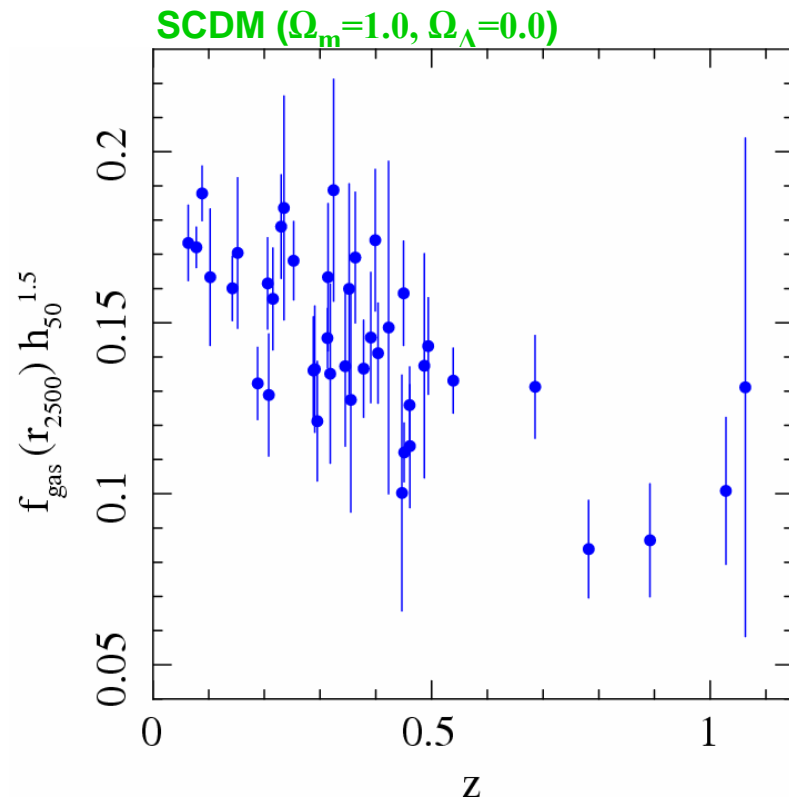
Simulations: Eke et al '98

Available **non-radiative** simulations for large ($kT > 5\text{keV}$) relaxed clusters suggest little/no evolution of bias factor within $0.5r_{\text{vir}}$ for $z < 1$.

So we expect the observed $f_{\text{gas}}(z)$ values to be approx. constant with z .

(See also Crain et al. 2007)

Chandra results on $f_{\text{gas}}(z)$



Brute-force determination of $f_{\text{gas}}(z)$ for two reference cosmologies:

→ Inspection clearly favours Λ CDM over SCDM cosmology.

To quantify: fit data with model which accounts for apparent variation in $f_{\text{gas}}(z)$ as underlying cosmology is varied → find best fit cosmology.

$$f_{\text{gas}}(z) = \frac{KA\gamma b(z)}{1+s(z)} \left(\frac{\Omega_b}{\Omega_m} \right) \left[\frac{d_A^{\text{LCDM}}(z)}{d_A^{\text{model}}(z)} \right]^{1.5}$$

Allowances for systematic uncertainties

Our full analysis includes a comprehensive and conservative treatment of potential sources of systematic uncertainty in current analysis.

1) The depletion factor (calibration, simulation physics, gas clumping etc.)

$$b(z) = b_0(1 + \alpha_b z) \quad \begin{array}{l} 20\% \text{ uniform prior on } b_0 \text{ (simulation physics)} \\ 10\% \text{ uniform prior on } \alpha_b \text{ (simulation physics)} \end{array}$$

2) Baryonic mass in stars: define $s = f_{\text{star}}/f_{\text{gas}} = 0.16h_{70}^{0.5}$

$$s(z) = s_0(1 + \alpha_s z) \quad \begin{array}{l} 30\% \text{ Gaussian uncertainty in } s_0 \text{ (observational uncertainty)} \\ 20\% \text{ uniform prior on } \alpha_s \text{ (observational uncertainty)} \end{array}$$

3) Non-thermal pressure support in gas: (primarily bulk motions)

$$\gamma = M_{\text{true}}/M_{\text{X-ray}} \quad 10\% \text{ uniform prior } 1 < \gamma < 1.1 \quad (\text{eg Nagai et al 2006})$$

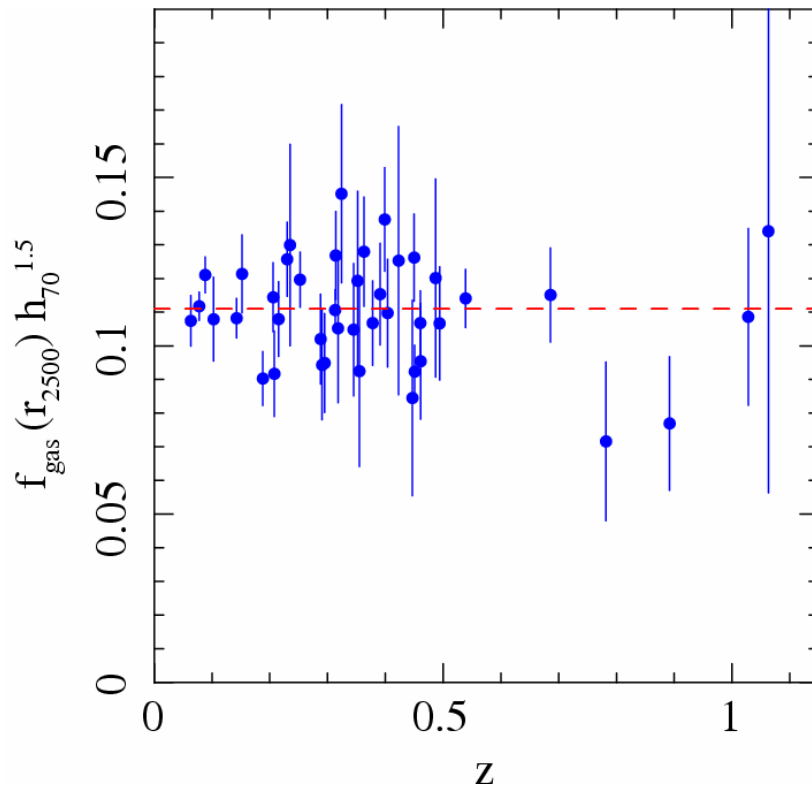
4) Instrument calibration, X-ray modelling

$$K \quad 10\% \text{ Gaussian uncertainty}$$

With these (conservative) allowances for systematics

Model:

$$f_{\text{gas}}(z) = \frac{KA\gamma b(z)}{1+s(z)} \left(\frac{\Omega_b}{\Omega_m} \right) \left[\frac{d_A^{\text{LCDM}}(z)}{d_A^{\text{model}}(z)} \right]^{1.5}$$



Results (Λ CDM)

Full allowance for systematics + standard priors:
($\Omega_b h^2 = 0.0214 \pm 0.0020$, $h = 0.72 \pm 0.08$)

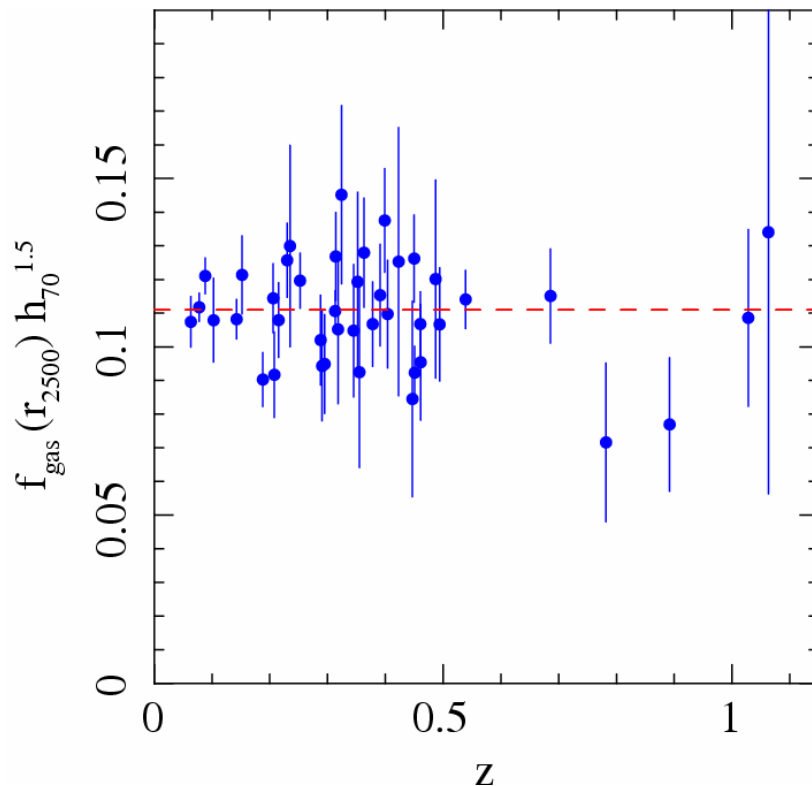
Best-fit parameters (Λ CDM):

$$\Omega_m = 0.27 \pm 0.06, \quad \Omega_\Lambda = 0.86 \pm 0.19$$

(Note also good fit: $\chi^2 = 41.5/40$)

↑
Important

The low systematic scatter in the $f_{\text{gas}}(z)$ data



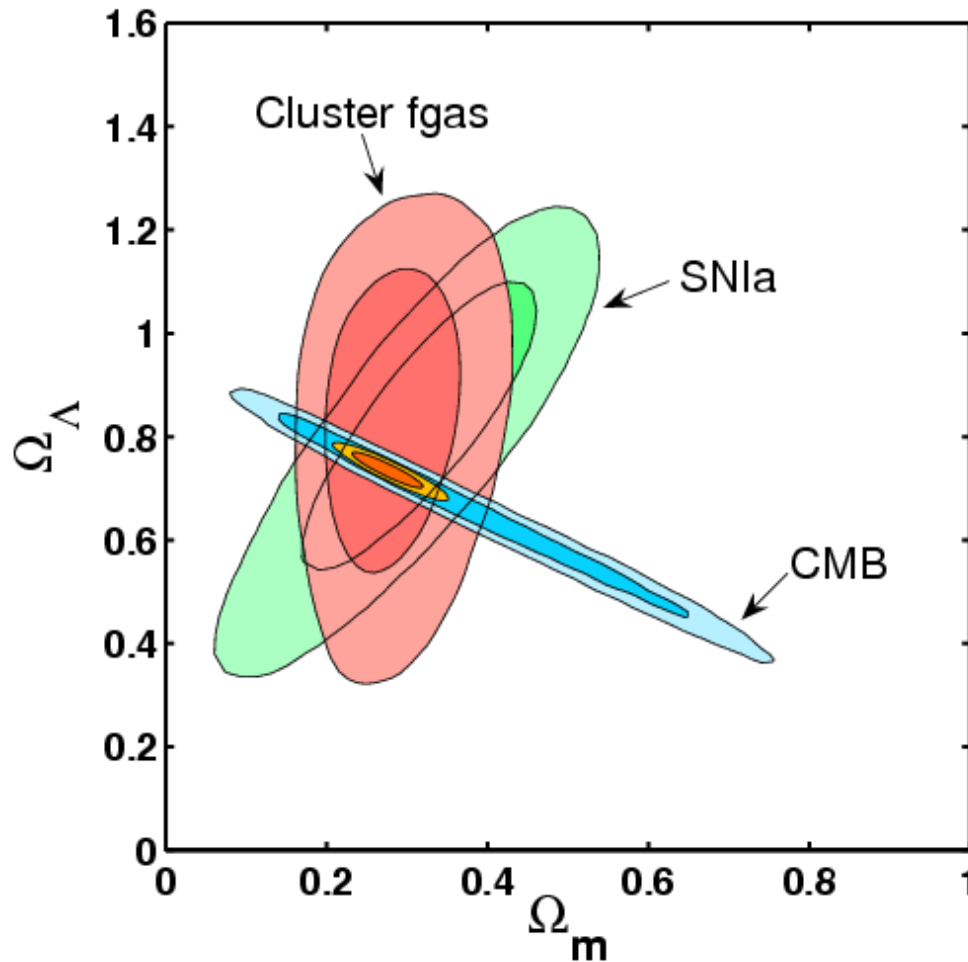
The χ^2 value is acceptable even though rms scatter about the best-fit model is only 15% in f_{gas} , or 10% in distance.

Weighted-mean scatter only 7.2% in f_{gas} or 4.8% in distance). c.f. SNIa, for which systematic scatter detected at $\sim 7\%$ level (distance).

Consistent with expectation from simulations (e.g. Nagai et al. '06)

The low systematic scatter in $f_{\text{gas}}(z)$ data offers the prospect to probe cosmic acceleration to high precision via absolute distance measurements, using the next generation of X-ray observatories (e.g. Constellation-X).

Comparison of independent constraints (Λ CDM)



f_{gas} analysis: 42 clusters including standard $\Omega_b h^2$, and h priors and full systematic allowances

CMB data (WMAP-3yr +CBI+ACBAR + prior $0.2 < h < 2.0$)

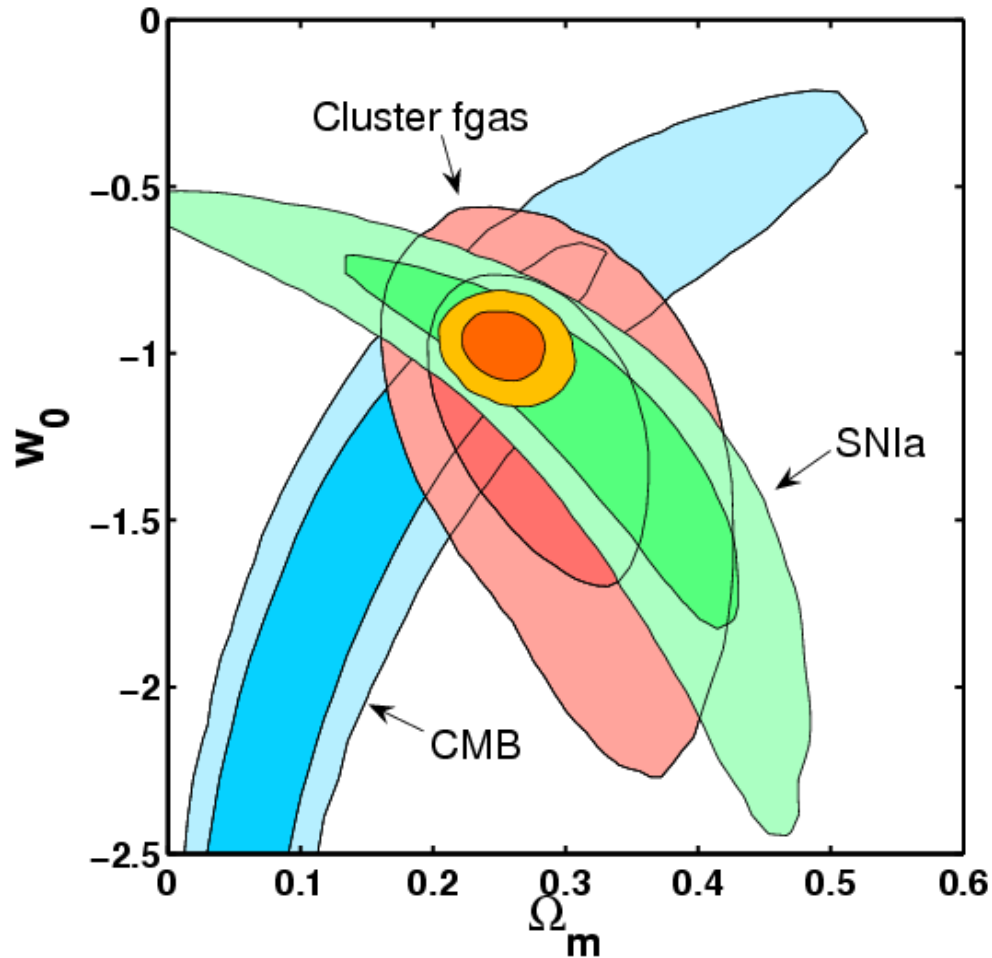
Supernovae data from Davis et al. '07 (192 SNIa, ESSENCE+SNLS+HST+nearby).

Combined constraint (68%)

$$\Omega_m = 0.275 \pm 0.033$$

$$\Omega_\Lambda = 0.735 \pm 0.023$$

Dark energy equation of state:



Constant w model:

Analysis assumes flat prior.

68.3, 95.4% confidence limits for all three parameter pairs consistent with each other.

Combined constraints (68%)

$$\begin{aligned}\Omega_m &= 0.253 \pm 0.021 \\ w_0 &= -0.98 \pm 0.07\end{aligned}$$

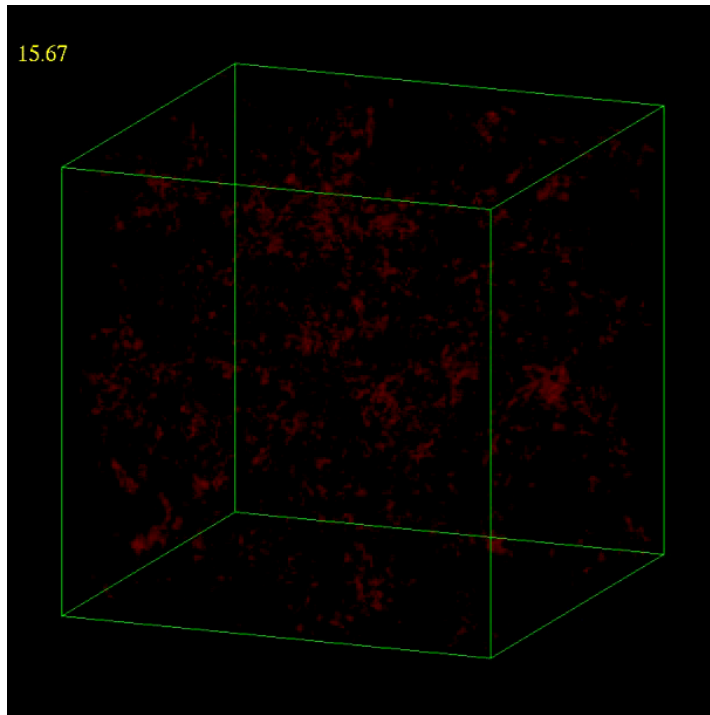
Probing cosmology with X-ray clusters

2b: The growth of cosmic structure (counting galaxy clusters as a function of redshift)

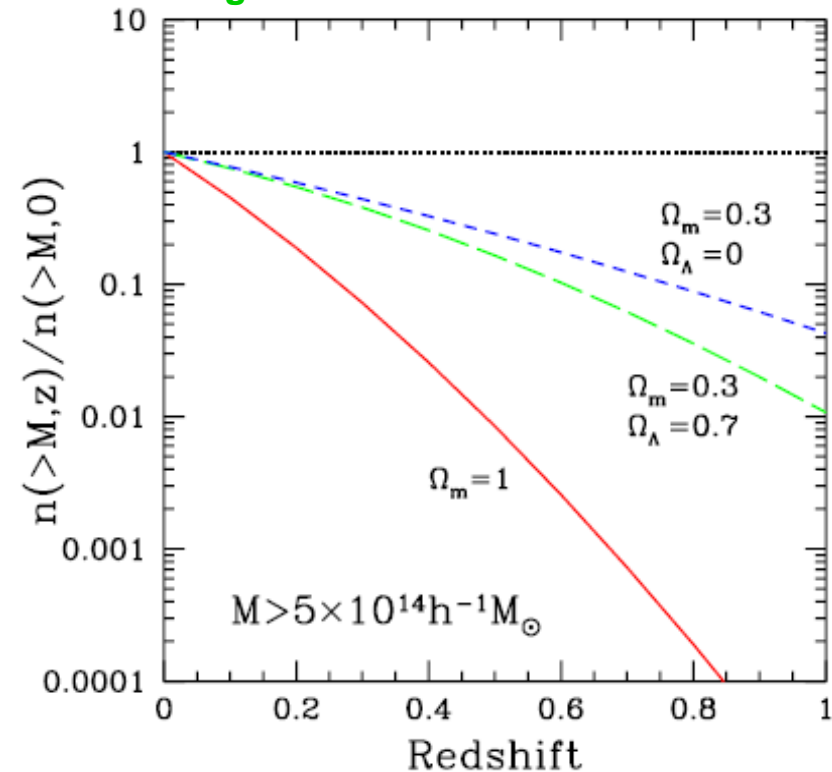
Mantz, Allen, Ebeling, Rapetti 2007, in preparation

Cluster growth of structure experiments

Moore et al.



Borgani '06



The observed growth rate of galaxy clusters provides (highly) complementary constraints on dark matter and dark energy to those from absolute distance measurements.

Ingredients for cluster growth of structure experiments

[THEORY] The predicted mass function for clusters, $n(M,z)$, as a function of cosmological parameters ($\sigma_8, \Omega_m, w_0, w_a$ etc) ← in hand from current + near future numerical simulations (e.g. Jenkins et al. '01)

[CLUSTER SURVEY] A large, wide-area, clean, complete cluster survey, with a well defined selection function.

Current leading work based on ROSAT X-ray surveys. Future important work based on new SZ (SPT, Planck) and X-ray (eROSITA/Spectrum-X-gamma) cluster catalogues (also optical and lensing surveys).

[SCALING RELATION] A tight, well-determined scaling relation between survey observable (e.g. L_x) and mass, with minimal intrinsic scatter.

Current best cluster surveys in X-rays

Low-redshifts ($z < 0.3$):

ROSAT Brightest Cluster Sample (BCS) (Ebeling et al. '98, '00). Based on RASS (northern sky). 201 clusters with $F_x > 4.4 \times 10^{-12} \text{ erg cm}^{-2} \text{ s}^{-1}$. 90% complete (100% redshift complete). 78 massive clusters with $L_x > 5 \times 10^{44} h_{50}^{-2} \text{ erg s}^{-1}$.

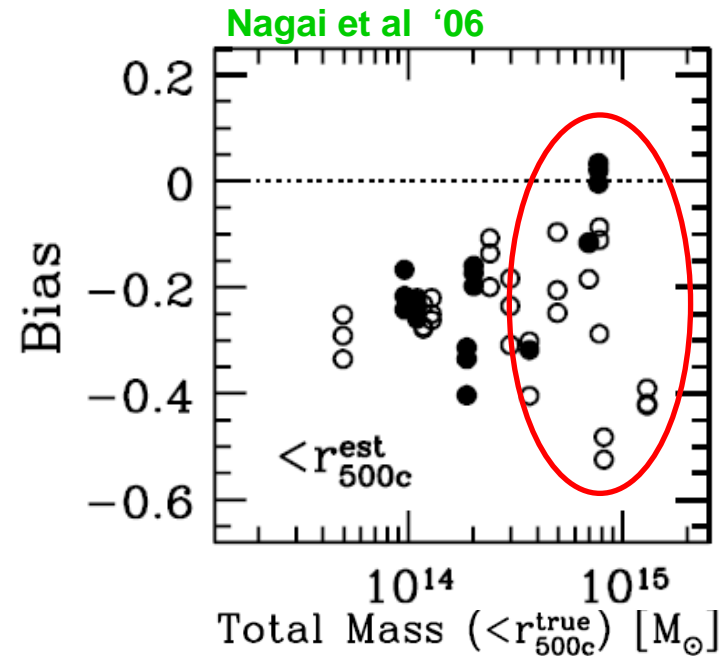
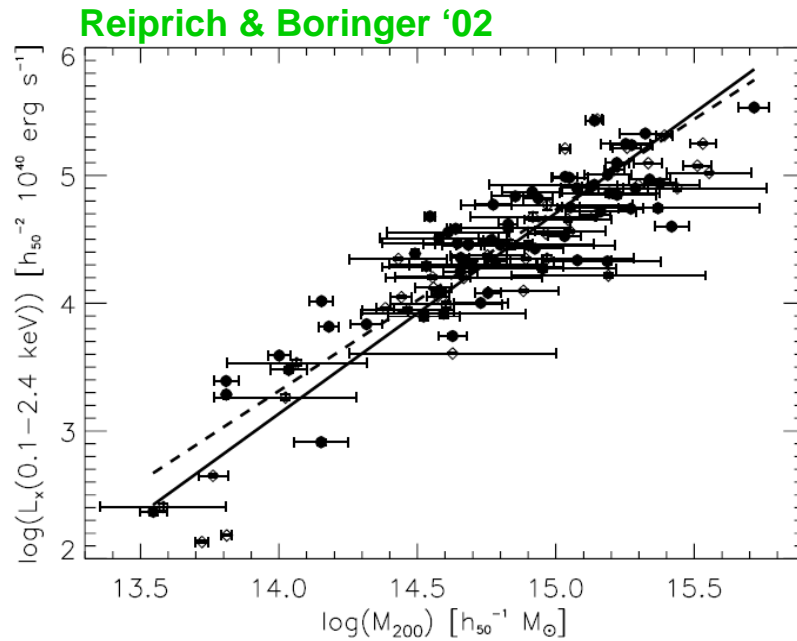
REFLEX (Bohringer et al '04). Based on RASS (southern sky). 447 clusters with $F_x > 3.0 \times 10^{-12} \text{ erg cm}^{-2} \text{ s}^{-1}$. ~100% complete (100% redshift complete). 130 massive clusters with $L_x > 5 \times 10^{44} h_{50}^{-2} \text{ erg s}^{-1}$ and $F_x > 3.0 \times 10^{-12} \text{ erg cm}^{-2} \text{ s}^{-1}$.

Intermediate redshifts ($0.3 < z < 0.7$):

MACS (Ebeling et al '01, '07). Based on RASS (whole sky: 23000 sq. deg). 124 clusters with $F_x > 10^{-12} \text{ erg cm}^{-2} \text{ s}^{-1}$. 34 massive clusters with $F_x > 2.0 \times 10^{-12} \text{ erg cm}^{-2} \text{ s}^{-1}$ and $L_x > 5 \times 10^{44} h_{50}^{-2} \text{ erg s}^{-1}$. ~100% complete (100% redshift complete).

ROSAT 400 sq. degree survey (Vikhlinin et al '07). ROSAT serendipitous cluster catalogue. 266 groups/small clusters with $F_x > 1.4 \times 10^{-13} \text{ erg cm}^{-2} \text{ s}^{-1}$. (100% redshift complete).

Current best scaling relations: X-ray luminosity and mass

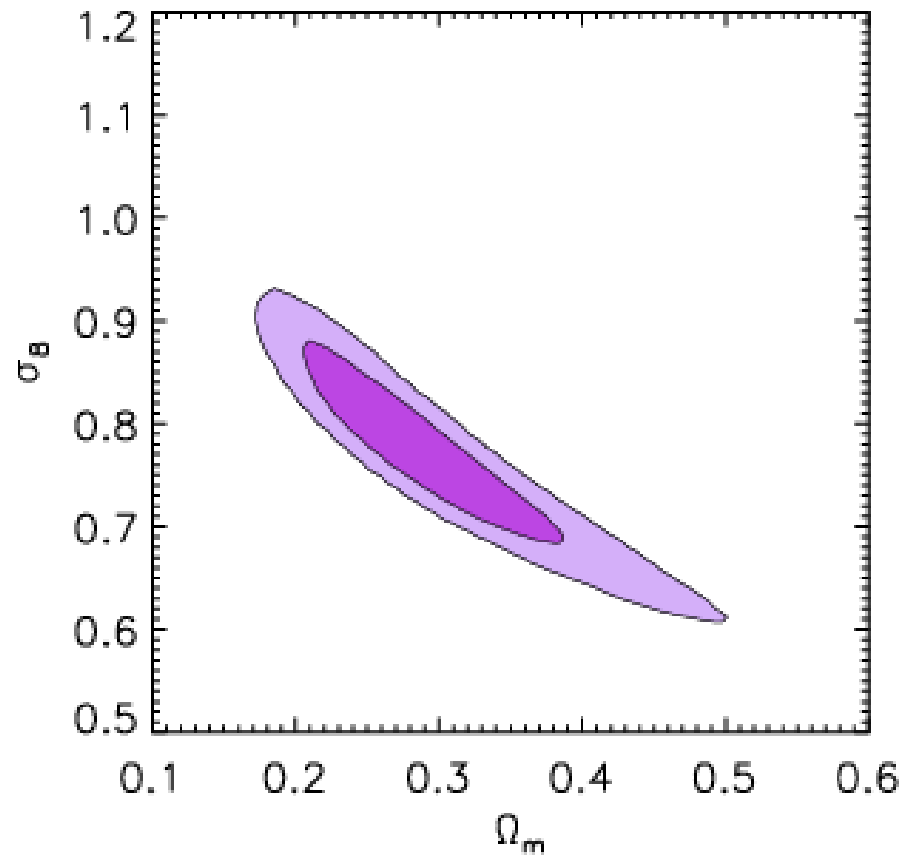


M, L both from X-ray observations. Major uncertainty is scale of bulk/turbulent motions in X-ray emitting gas. Can correct for this using hydro. simulations.

Based on sims assume bias -25% and scatter $\pm 15\%$ due to bulk motions (dominant systematic uncertainty). Also allow for $\pm 10\%$ evolution.

Alternatively, can measure masses via gravitational lensing. Independent method with very different uncertainties. Work is underway....

Results on σ_8 , Ω_m



Flat Λ CDM model:

REFLEX+BCS+MACS ($z < 0.7$).
242 clusters, $L_x > 5e44$ erg/s.
2/3 sky. $n(M, z)$ only.

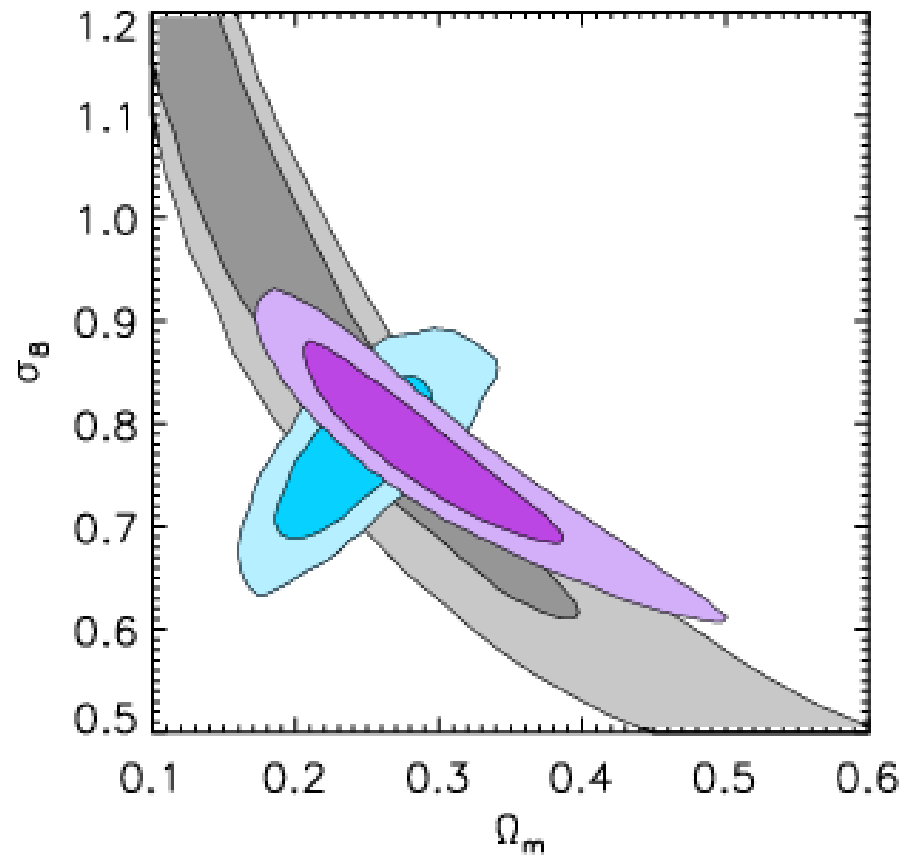
68.3, 95.4% confidence limits

Marginalized constraints (68%)

$$\Omega_m = 0.28 \pm 0.06$$

$$\sigma_8 = 0.77 \pm 0.07$$

Comparison with best other current results on σ_8 , Ω_m



Flat Λ CDM model:

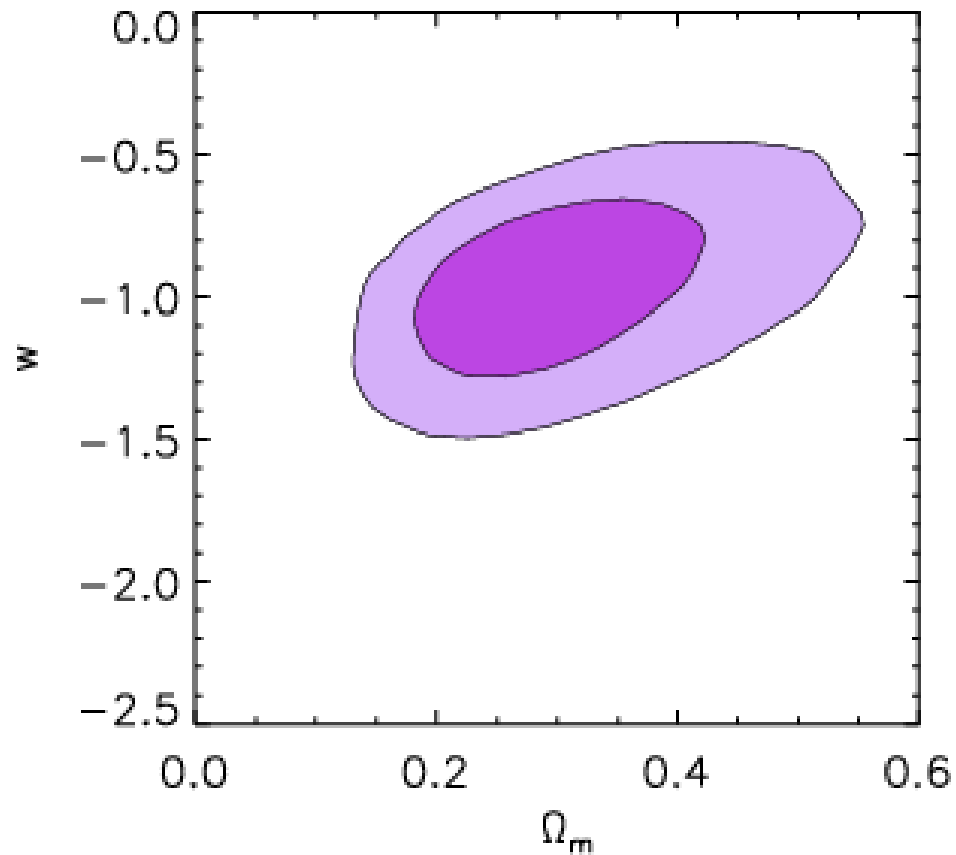
X-ray cluster number counts
(Mantz et al. '07)

CMB data (WMAP3)

Cosmic Shear (weak lensing)
100 square degree survey
(Benjamin et al. '07)

68.3, 95.4% confidence
limits shown in all cases.

Results on dark energy



Flat, constant w model:

REFLEX+BCS+MACS ($z < 0.7$).
242 clusters, $L_x > 5e44$ erg/s.
2/3 sky. $n(M, z)$ only.

68.3, 95.4% confidence limits

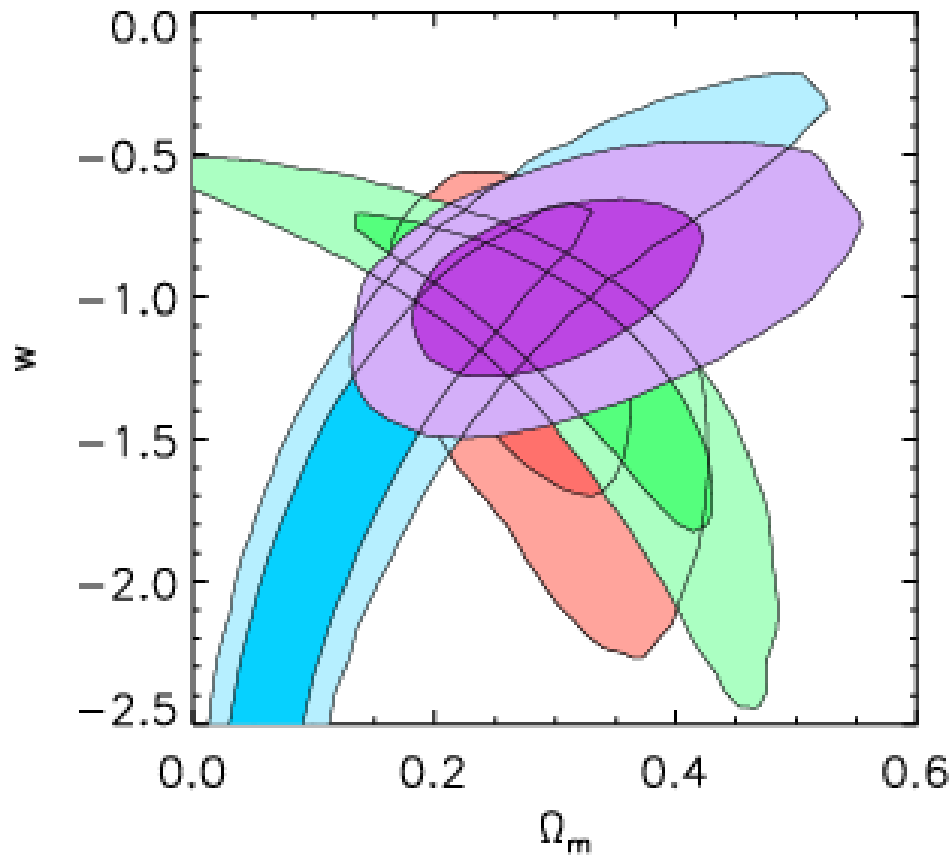
Marginalized constraints (68%)

$$\Omega_m = 0.27 \pm 0.07$$

$$\sigma_8 = 0.75 \pm 0.08$$

$$w = -0.95 \pm 0.20$$

Comparison with best other results on dark energy



Flat, constant w model:

X-ray cluster number counts
(Mantz et al. '07)

X-ray cluster f_{gas} analysis
(Allen et al '07)

CMB data
(WMAP-3yr +CBI+ACBAR)

SNIa data (Davis et al. '07
(192 SNIa, ESSENCE+
SNLS+HST+nearby).

Excellent agreement between completely independent techniques. All data consistent with cosmological constant ($w = -1$) model.

Conclusions

The NFW model provides a good description of the dark matter profiles in the largest, relaxed galaxy clusters. The overall shapes, innermost density profiles and observed concentration-mass relation are all in good agreement with predictions for the standard cold dark matter model.

$f_{\text{gas}}(z)$ data for largest relaxed clusters \rightarrow tight constraints on Ω_M , Ω_Λ and w via absolute distance measurements.

$$\Omega_M = 0.27 \pm 0.06 \quad \Omega_\Lambda = 0.86 \pm 0.19 \quad w = -1.14 \pm 0.31$$

Measurements of the growth of X-ray luminous clusters spanning $0 < z < 0.7 \rightarrow$ tight, independent constraints on Ω_M , σ_8 and w .

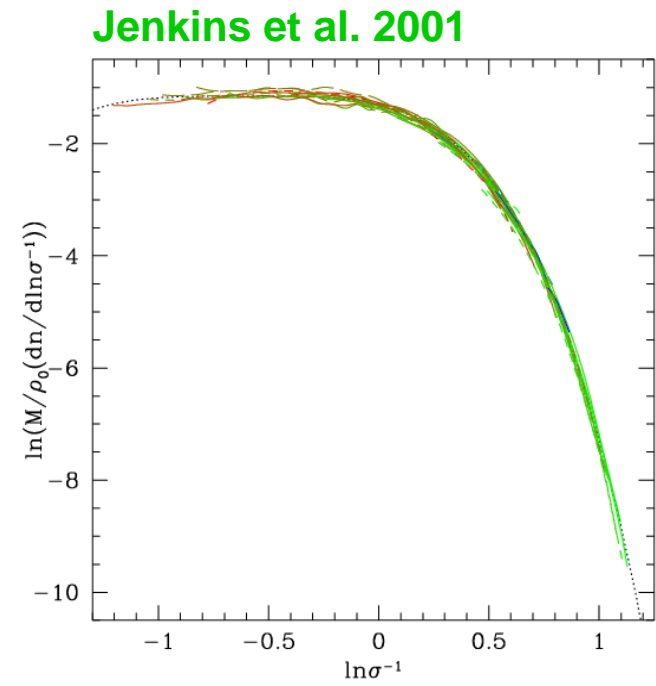
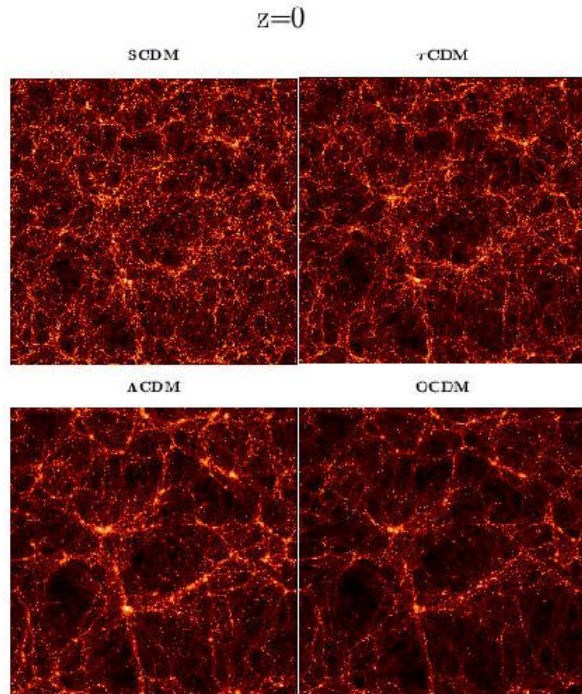
$$\Omega_M = 0.27 \pm 0.07 \quad \sigma_8 = 0.75 \pm 0.08 \quad w = -0.95 \pm 0.20 \text{ (flat model)}$$

(Note: combination of distance and growth of structure experiments is likely to provide key to distinguishing dark energy from modified gravity models.)

Extra slides (not shown)

The predicted mass function of cluster halos

The mass function of halos is independent of the background cosmology.



$$f(M) = \frac{M}{\bar{\rho}} \frac{dn(M, z)}{d \ln \sigma^{-1}} = A \exp(-|\ln \sigma^{-1} + B|^\epsilon)$$

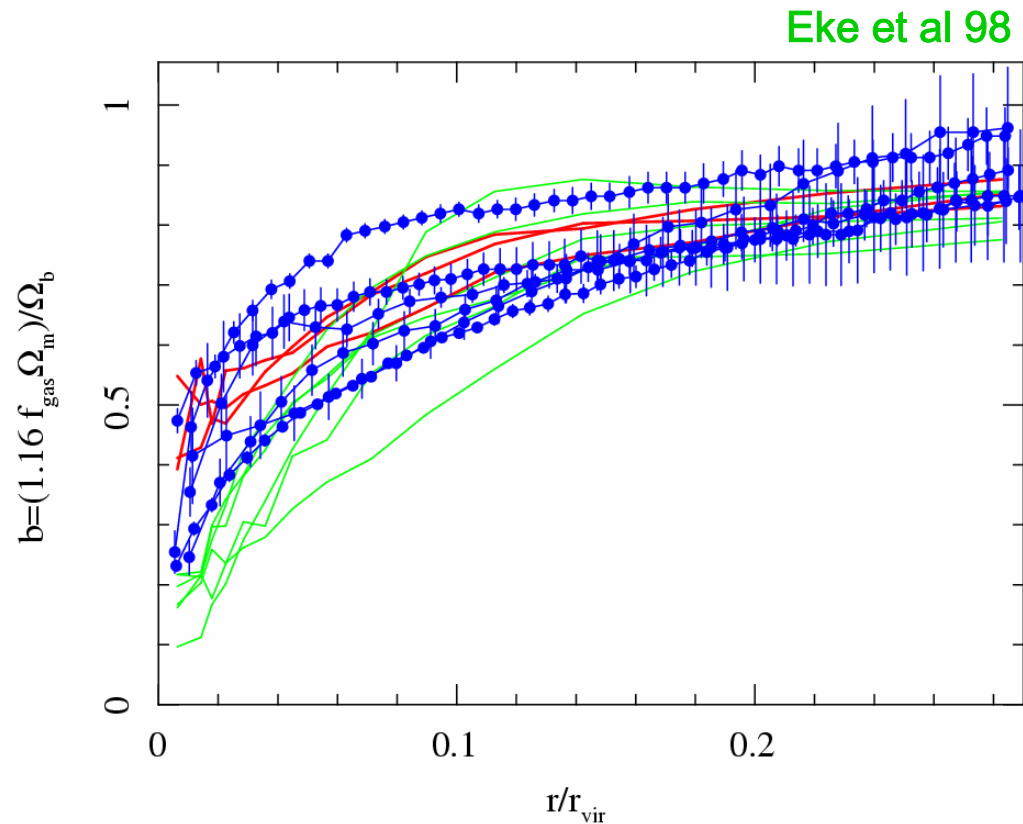
A, B, ϵ constants.
 $\sigma(M, z)$ scales with linear growth factor
(Jenkins et al '01)

Comparison of observed and simulated fgas profiles

Simulations:

$$f_{\text{baryon}} = b \frac{\Omega_b}{\Omega_m}$$

Result is challenging for MOND or TeVeS theories with no dark matter.



Good agreement with non-radiative simulations.

New large hydro simulations (based on Millenium run) including wide range of plausible gas physics underway (Thomas, Kay, Pearce et al.). Should significantly reduce uncertainties associated with $b(z)$.